

Electrostatic modification of novel materials

C. H. Ahn

Department of Applied Physics, Yale University, New Haven, Connecticut 06520–8120, USA

A. Bhattacharya

Argonne National Laboratory, 9700 S. Cass Ave., Argonne, Illinois 60439, USA

M. Di Ventra

Department of Physics, University of California San Diego, La Jolla, California 92093, USA

J. N. Eckstein

Department of Physics, University of Illinois at Urbana-Champaign, Urbana, Illinois 61801, USA

C. Daniel Frisbie

Department of Chemical Engineering and Materials Science, University of Minnesota, Minneapolis, Minnesota 55455, USA

M. E. Gershenson

Department of Physics and Astronomy, Rutgers, the State University of New Jersey, Piscataway, New Jersey 08854, USA

A. M. Goldman

School of Physics and Astronomy, University of Minnesota, Minneapolis, Minnesota 55455, USA

I. H. Inoue

Correlated Electron Research Center, National Institute of Advanced Industrial Science and Technology, AIST Tsukuba Central, Tsukuba, Japan

J. Mannhart

Experimentalphysik VI, Center for Electronic Correlations and Magnetism, Institute of Physics, Augsburg University, D-86135 Augsburg, Germany

Andrew J. Millis

Department of Physics, Columbia University, New York, New York 10027, USA

Alberto F. Morpurgo

Kavli Institute of Nanoscience, Delft University, Lorentzweg 1, 2628 CJ Delft, The Netherlands

Douglas Natelson

Department of Physics and Astronomy, Rice University, Houston, Texas 77005, USA

Jean-Marc Triscone

Ecole de Physique, Département de Physiques de la Matière Condensée, 24 quai Ernest-Ansermet, 1211 Genève 4, Switzerland

(Published 10 November 2006)

Application of the field-effect transistor principle to novel materials to achieve electrostatic doping is a relatively new research area. It may provide the opportunity to bring about modifications of the electronic and magnetic properties of materials through controlled and reversible changes of the carrier concentration without modifying the level of disorder, as occurs when chemical composition is altered. As well as providing a basis for new devices, electrostatic doping can in principle serve as a tool for studying quantum critical behavior, by permitting the ground state of a system to be tuned in a controlled fashion. In this paper progress in electrostatic doping of a number of materials systems is reviewed. These include structures containing complex oxides, such as cuprate superconductors and colossal magnetoresistive compounds, organic semiconductors, in the form of both single crystals and

thin films, inorganic layered compounds, single molecules, and magnetic semiconductors. Recent progress in the field is discussed, including enabling experiments and technologies, open scientific issues and challenges, and future research opportunities. For many of the materials considered, some of the results can be anticipated by combining knowledge of macroscopic or bulk properties and the understanding of the field-effect configuration developed during the course of the evolution of conventional microelectronics. However, because electrostatic doping is an interfacial phenomenon, which is largely an unexplored field, real progress will depend on the development of a better understanding of lattice distortion and charge transfer at interfaces in these systems.

DOI: [10.1103/RevModPhys.78.1185](https://doi.org/10.1103/RevModPhys.78.1185)

PACS number(s): 73.90.+f, 72.90.+y, 73.43.Nq

CONTENTS

I. Introduction	1186
II. Conventional MOSFETs	1187
III. Correlated Oxide Compounds	1189
A. Enabling experiments and technologies	1189
B. Scientific issues and challenges	1193
IV. Organic Semiconductors	1195
A. Enabling experiments and technologies	1195
B. Scientific issues and challenges	1196
V. Inorganic Layered Semiconductors	1199
VI. Single Molecules	1200
A. Enabling experiments and technologies	1200
B. Scientific issues and challenges	1203
VII. Magnetic Semiconductors	1206
VIII. Future Research Opportunities	1207
IX. Discussion	1209
Acknowledgments	1209
References	1209

I. INTRODUCTION

Silicon semiconducting field-effect transistors (FETs) are ubiquitous in microelectronics, with $\sim 10^{18}$ FETs being manufactured every year (Ahn *et al.*, 2003). Applying the FET principle to new materials offers appealing prospects, and electrostatic modulation of the carrier density in novel materials can lead not only to changes in resistivity but at a deeper level to modification of the fundamental electronic properties of materials. These perspectives and ongoing efforts on the field effect in several materials systems will be discussed in this review. The usual approach to properties modification involves changing chemical composition (chemical doping). This approach, although very successful, has two drawbacks: it is not tunable (essentially a new sample must be created for each doping level desired), and in general changing chemical composition induces disorder or alters the level of disorder. Electrostatic doping is an attractive alternative as it allows, in principle, controlled and reversible changes of the carrier concentration without altering the level of disorder in the material. It is now becoming possible to electrostatically add carriers to materials other than conventional semiconductors at a level that can have a significant effect on material properties.

Figure 1 illustrates several of the material properties as a function of their sheet charge density (Ahn *et al.*, 2003). In many of the thin-film and single-crystal mate-

rials of interest the electrostatic screening lengths are short (of the order of a lattice constant), so that the induced charge remains within one or two unit cells of the interface. This is a result of the relatively high carrier densities in these materials. For correlated oxides such as high- T_c superconductors and manganites, where lattice constants are of the order of 4 Å, one electron per unit cell corresponds to an areal density of $6 \times 10^{14}/\text{cm}^2$. Reference to the phase diagrams of correlated systems (Imada, Fujimori, and Tokura, 1998) suggests that to electrostatically induce phase transitions it is typically necessary to change electron concentrations by an amount of the order of 0.1–0.3 electron per unit cell. However, if materials are fine-tuned to the close proximity of a critical point, much smaller changes in carrier concentration would suffice. In organic compounds the unit cells are larger and interesting phenomena may occur at relatively low charge transfers. It is now technically possible to supply a level of charge transfer of $(1-3) \times 10^{14}/\text{cm}^2$ or about 0.3 carrier per unit cell to the surface region of several novel materials, using either the surface charge of a high dielectric constant material (Mannhart, 1996) or of a ferroelectric (Ahn *et al.*, 1999). In the case of cuprates, which are of particular interest, changing the density by ~ 0.2 electron per unit cell would convert a material from an antiferromagnetic insulator with a 2-eV gap to a superconductor with a transition temperature of ~ 100 K. Recent experiments (Ahn *et al.*, 1999) have demonstrated changes in electronic properties corresponding to modulations of mobile carrier density of $\sim 10^{14}$ charges/ cm^2 , indicating that charges of this density have been added to electron levels relevant to superconductivity, rather than to trap states. As a consequence, significant modulation of electronic properties has already been demonstrated. The status of electrostatic doping of the following materials systems will be discussed in this review: (1) complex oxides such as cuprate superconductors and colossal magnetoresistance compounds, which demonstrate remarkable correlation physics depending upon carrier concentration; (2) organic semiconductors, both in single crystals and in thin films (Jerome and Caron, 1987; IBM, 2001); (3) layered inorganics (Podzorov *et al.*, 2004a, 2004b), where the basic physics of electrical conduction and carrier injection is largely not understood; (4) single-molecule devices where the field effect allows one to tune molecular levels and examine a host of interesting physics issues as a function of such a tuning parameter, and for completeness; and (5) magnetic semiconductors,

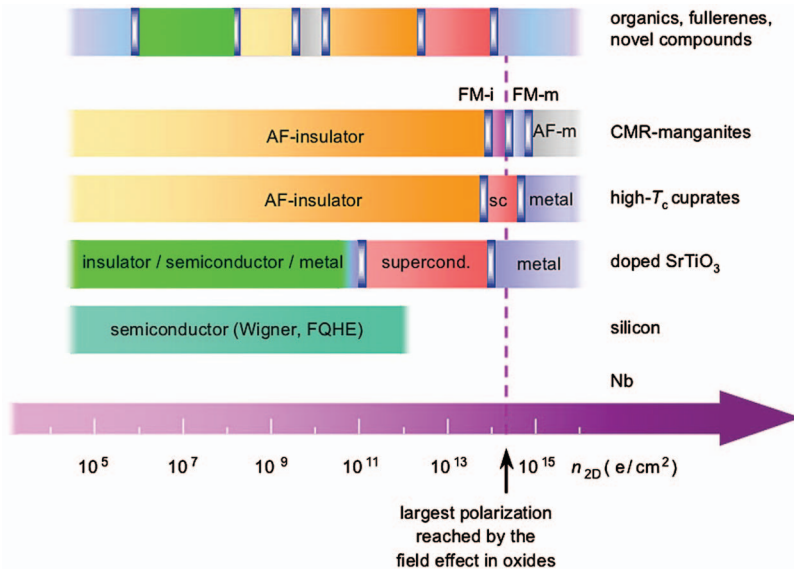


FIG. 1. (Color) Illustration of the zero-temperature behavior of various correlated materials as a function of sheet charge density. Silicon is shown as a reference. The examples for high-temperature superconductors and for colossal magnetoresistive manganites reflect $\text{YBa}_2\text{Cu}_3\text{O}_7$ and $(\text{La}, \text{Sr})\text{MnO}_3$, respectively. Top bar shows schematically the richness of materials available for field-effect tuning and the spectrum of their phases. AF, FM, I, M, SC, FQHE, and Wigner stand for anti-ferromagnetic, ferromagnetic, insulator, metal, superconductor, fractional quantum Hall effect, and Wigner crystal, respectively. From Ahn *et al.*, 2003.

where electrostatic charging has been used to tune magnetization. In this paper we discuss enabling experiments and the scientific and technological opportunities. For some of the systems considered in this review, results can be anticipated by employing earlier knowledge of materials and devices, drawing on what was learned in the development of microelectronics. However, fundamentally new issues are likely to arise. Electrostatic doping is a surface effect, and much remains to be understood about surface properties of complex materials. Furthermore, as presented in Sec. II.B, for the systems discussed here the injected charge is concentrated within one to three unit cells of the interface with the gate insulator (in contrast with semiconductor FETs, which are characterized by screening lengths of hundreds of angstroms or more), leading to large gradients in the charge density and thus in the electrical potential. Depending upon the materials system, gradients of the areal carrier density of $10^{20}/\text{cm}^2/\text{cm}$ may be reached. It seems very likely that the physics of this situation will differ in many ways from the physics of bulk materials. Finally, unlike conventional compounds, in complex materials electrostatic doping can alter fundamental properties of the electronic system, by inducing phase transitions (thereby, for example, forming or destroying an energy gap at the Fermi level) or less dramatically by changing the value of magnetic or superconducting transition temperatures. We begin with a review of the operation of conventional FETs, to provide a baseline for our discussion of the new effects which may be induced by electrostatic charging of novel materials.

II. CONVENTIONAL MOSFETs

In semiconductor field-effect devices such as MOSFETs (metal-oxide-semiconductor field-effect transistors), the geometry consists of source and drain terminals, a conducting channel between them, and a gate terminal that modulates the conductance of this channel (Sze, 1981). The channel could be, for example, a thin

layer at the surface of a doped semiconductor, a thin film of semiconducting material, or a two-dimensional electron gas in a quantum well. Ideally, the source and drain contacts to the channel should be low resistance and Ohmic. The gate electrode and channel are isolated from one another by an insulating dielectric and form two electrodes of a parallel plate capacitor. Application of a voltage (V_G) across this capacitor induces charge into the channel near the semiconductor-dielectric interface. The electric field penetrating the semiconductor causes the energy spectrum of the states near the interface to shift (band bending). This changes the relative position of the Fermi level with respect to the delocalized bands, changing the density of mobile carriers and the conductance of the interfacial region. Depending upon the direction and extent of the shift in the energy levels induced by the gate, the carrier density of the interfacial region can be enhanced (accumulation), reduced (depletion), or reversed in sign (inversion) compared to the density in the bulk. This is illustrated in Fig. 2. The carrier density in the bulk of a doped semiconductor is typically 10^{17} – $10^{18}/\text{cm}^3$, and this translates to an areal carrier density of 10^{12} – $10^{13}/\text{cm}^2$ for a channel thickness of 100 \AA . Changes in carrier density of the order of 10^{12} – $10^{13}/\text{cm}^2$ can be induced in the channel by a gate before dielectric breakdown occurs in typical dielectrics like SiO_2 , and densities in excess of $10^{14}/\text{cm}^2$ have been obtained using SrTiO_3 and ferroelectrics such as lead zirconate titanate (PZT). This may be much larger than the carrier density in the material itself, causing large changes in conductance. The ratio of currents in the presence and absence of a gate voltage is often referred to as the on-off ratio. In many instances, the induced charge initially populates localized states, and no change in the channel conductance is obtained until a threshold voltage V_T is reached. The value of this threshold depends upon factors such as the density of localized states in the semiconductor, traps at the oxide-semiconductor interface, and immobile charges or defects in the dielectric.

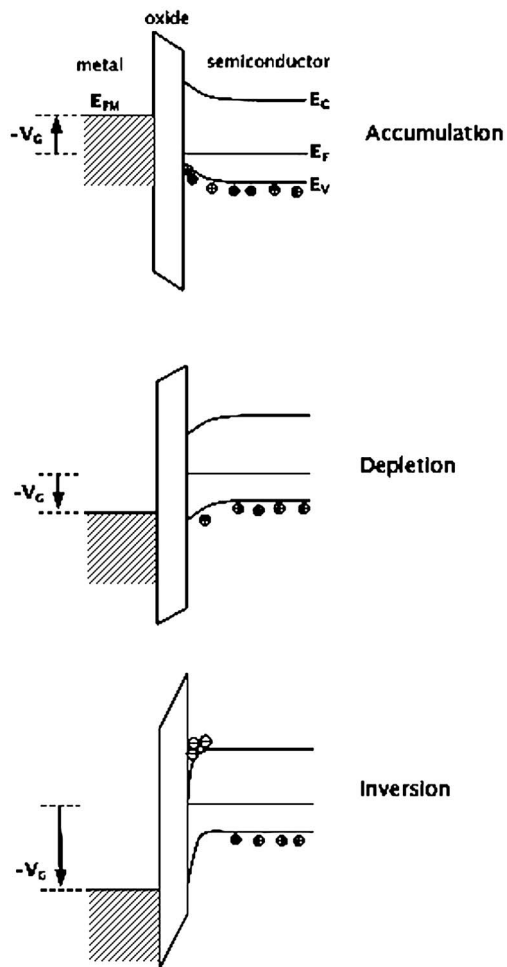


FIG. 2. Accumulation, depletion, and inversion at an MOS interface: the left side shows the gate voltage with the conduction electrons of the gate shown by the shaded region. Energy is plotted vertically. On the right side are shown the bands in the semiconductor, with doping producing hole-type carriers in the lower band. The accumulation and depletion conditions show increased and decreased carrier density at the interface. Under inversion conditions electron carriers appear in the upper band.

The current-voltage characteristics of a MOSFET may be understood in terms of Shockley’s gradual channel model for the conducting channel, where the density of carriers is modulated by the gate voltage V_G . In the presence of a bias voltage between the source and drain (V_D), the charge density induced by the gate at a given point in the channel depends upon the local channel potential $V_C(x)$ [$0 < V_C(x) < V_D$]. In the limit where the potential in the channel varies very little over lengths on the order of the insulator thickness, the current at a point in the channel may be expressed as

$$I_D = \mu C_L [(V_G - V_T) - V_C(x)] W \frac{dV_C(x)}{dx}, \quad (1)$$

where x is a coordinate along the length of the channel, μ is the carrier mobility, C_L is the capacitance per unit area of the gate insulator, and W is the width of the channel. Upon integrating this expression over the

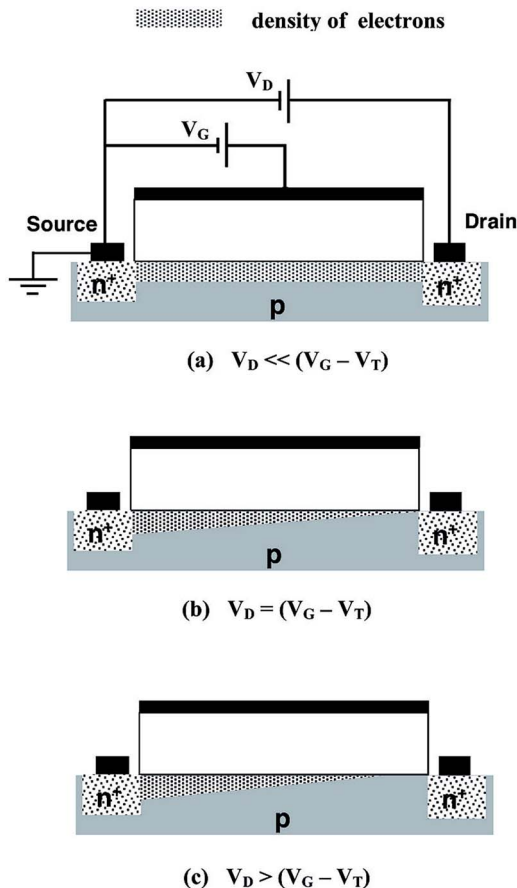


FIG. 3. (Color online) MOSFET on a p -type (hole-doped) substrate, with the conducting channel being an inversion layer of electrons. The source and drain contacts are made through heavily doped n -type (electron-doped) regions that ensure Ohmic contact through a very thin Schottky barrier. The three stages of operation are (a) linear, (b) near pinch-off, and (c) in saturation.

length L of the channel, we obtain an expression for the current-voltage characteristic,

$$I_D = \mu C_L [(V_G - V_T) V_D - V_D^2/2] \frac{W}{L}. \quad (2)$$

At small source-drain bias, where $V_D \ll V_G - V_T$, the I_D vs V_D curves are linear, with a slope proportional to $V_G - V_T$. At higher bias, as V_D approaches $V_G - V_T$, the density of carriers induced near the drain electrode gets depleted to zero, a condition known as “pinch off.” At higher values of V_D , the undepleted length of the channel where there are free carriers becomes shorter, but the accompanying lower carrier density causes the integrated resistance of this region to remain unchanged. In the depleted region of the channel, the carriers are swept into the drain by a longitudinal electric field that exactly compensates for the energy barrier seen by the carriers in the depleted region. Thus the I_D vs V_D curve becomes flat, or saturates. (See Fig. 3 for a cartoon of the stages of operation.)

Typically, the mobility of carriers in saturation may be different from that in the linear regime. In this regime,

the I_D vs V_D curve is assumed to remain constant at the maximum value that can be attained by Eq. (2), when $V_D = V_G - V_T$,

$$I_{D\text{sat}} = \mu C_I \left[\frac{(V_G - V_T)^2}{2} \right] \frac{W}{L}. \quad (3)$$

From Eq. (2) at low bias, and Eq. (3), values of linear and saturation mobility may be extracted. Curves of I_D vs V_D calculated from the above equations are shown in Fig. 4. This treatment does not take into account the effects of the variation in $V_C(x)$ on the position of the bands relative to the Fermi energy (band bending) along the channel. This and other effects relevant to modern MOSFETs such as short-channel effects are treated in many standard texts (Sze, 1981; Shur, 1990). It will be seen in what is presented in subsequent sections that additional physics may be relevant to the development of an understanding of field-effect doping of novel materials.

III. CORRELATED OXIDE COMPOUNDS

A. Enabling experiments and technologies

The study of correlated oxide compounds has been an active area of research for some time (Imada, Fujimori, and Tokura, 1998; Tokura, 2000). The main scientific drivers are the multiplicity of new and interesting effects (for example, high-temperature superconductivity and “colossal” magnetoresistance) and the observation that many of the ideas central to the understanding of simple metals and semiconductors seemingly fail, indicating the need for new theoretical and experimental approaches. It is not our purpose here to air all of the open questions in this field, but to focus on the opportunities for progress offered by the electrostatic charging technique.

A generic feature of correlated electron systems is the close competition of two or more electronic phases with small changes in chemical composition, strain, or external fields changing the system (or a small region of the system) from one to the other (Millis, 2003). This motivates research on FET configurations with the goal of employing electrostatic modification with charge density as a tuning parameter. Succeeding with electrostatic doping would open up opportunities for fundamental investigations and might also lead to novel devices. With the long history of advances in the growth of thin-film oxides and the enormous diversity of compounds and properties, there is a huge phase space that might be explored.

For oxides with complex electronic properties that are embedded in heterostructures, new issues of physics, chemistry, and materials science also arise. The presence of the interface is known to affect the chemical and electronic environment strongly (Altieri *et al.*, 2002), that can change basic electronic parameters, such as the Hubbard energy U , the electronic bandwidths, or the exchange energies. These can furthermore be altered by applying a polarization via the gate electrode. In addi-

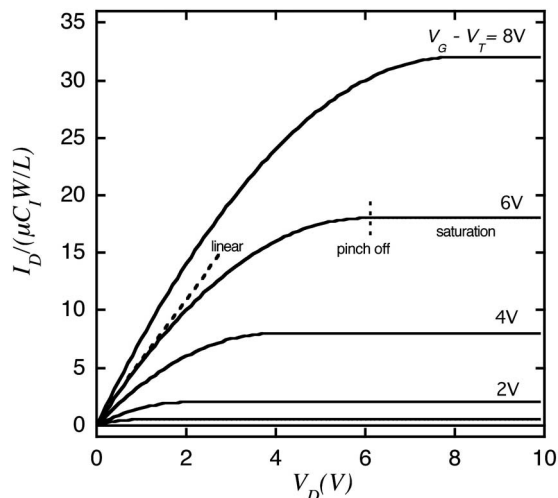


FIG. 4. I_D - V_D curves calculated from the equations in the text. The linear (low V_D) regime, pinch-off, and saturation are indicated for the $V_G - V_T = 6$ V curve.

tion, gating can create charge density gradients of unprecedented magnitudes (Ahn *et al.*, 1999; Okamoto and Millis, 2004a); the effects of these on the behavior of interest must be understood. Further, the field-induced phases are not neutral, but electrically charged, and may therefore display uncommon properties.

In this section we describe a few recent studies which show that interesting levels of electrostatic doping are achievable in high-temperature superconductors, colossal magnetoresistive materials, and oxide channel field-effect transistors. The studies we describe have all relied on the use of evaporated dielectric oxides as the insulator, on altering the polarization of a deposited ferroelectric compound to effect change in the surface carrier concentration, or on the use of thinned single-crystal substrates with high dielectric constants in a manner that combines the gate insulator with the substrate. A complementary approach is to use the rapidly developing techniques of oxide epitaxy (Izumi *et al.*, 2001) to engineer at the atomic level interfaces with the desired properties. For example, Ohtomo *et al.* (2002) have demonstrated the fabrication of atomically precise $(\text{LaTiO}_3)_3(\text{SrTiO}_3)_m$ multilayers comprised of a controllable number $n=1,2,3,\dots$ of (001) layers of the nearly ferroelectric material SrTiO_3 (see Fig. 5). These authors have presented longitudinal and Hall resistance data showing that the structures (although comprised of two insulators) are metallic for $n < 7$, and have used TEM and electron-energy-loss spectroscopy (EELS) techniques to investigate the variation of the Ti d -electron density across the structures (see Fig. 6). Qualitatively similar heterostructures involving colossal magnetoresistance manganites (Warusawithana *et al.*, 2003; Oh *et al.*, 2004; Bhattacharya *et al.*, 2005) and high- T_c superconductors (Bozovic *et al.*, 2004) are now becoming available. These new classes of materials make possible controlled studies of interface effects in correlated materials.

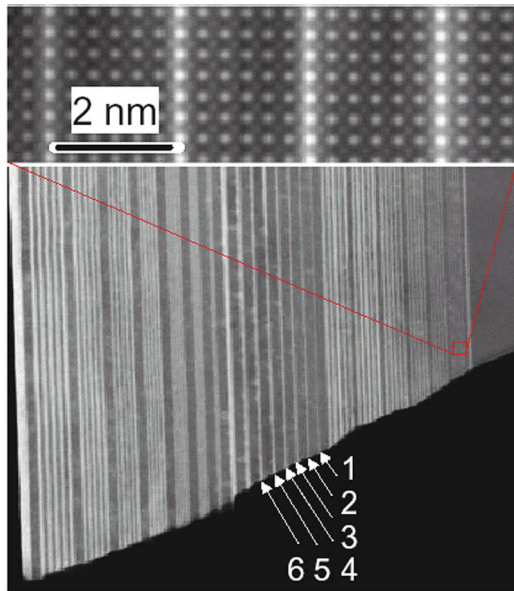


FIG. 5. (Color online) Dark-field image of LaTiO_3 layers (bright lines) of varying thickness separated by varying thicknesses of SrTiO_3 (darker regions) layers. The view is along the $[100]$ zone axis of the SrTiO_3 substrate which is the dark region on the right. After the deposition of calibration layers, the growth sequence is $5 \times n$, 5 layers of SrTiO_3 and n layers of LaTiO_3 , $20 \times n$, $n \times n$, and finally a capping layer of LaTiO_3 . The numbers in the image indicate the number of LaTiO_3 unit cells in each layer. The total field of view is 400 nm. Upper panel: magnified view of the 5×1 region. From [Ohtomo *et al.*, 2002](#).

We begin with experiments on high-temperature superconductors ([Bednorz and Müller, 1986](#)). To understand the prospects for electrostatic doping of high-

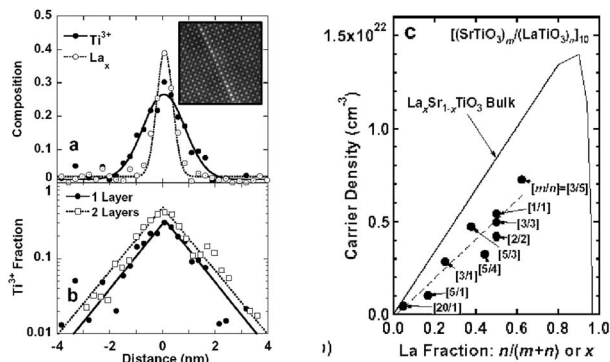


FIG. 6. Charge modulation in atomic scale $\text{LaTiO}_3/\text{SrTiO}_3$ heterostructures. Left panel: Top shows the variation of the electron energy-loss spectra for La and Ti across a single LaTiO_3 layer. Inset: The image of this single layer corresponding to layer 1 in Fig. 5. The Ti signal is considerably wider than that of the La. The lower panel on the left shows the decay of the Ti signal away from monolayers and bilayers of LaTiO_3 . (In bulk this is 0 for SrTiO_3 and 12 for LaTiO_3 .) Right panel: Carrier density from Hall resistivity for a variety of heterostructures, showing interface-induced metallic behavior from a mixture of two insulating components.

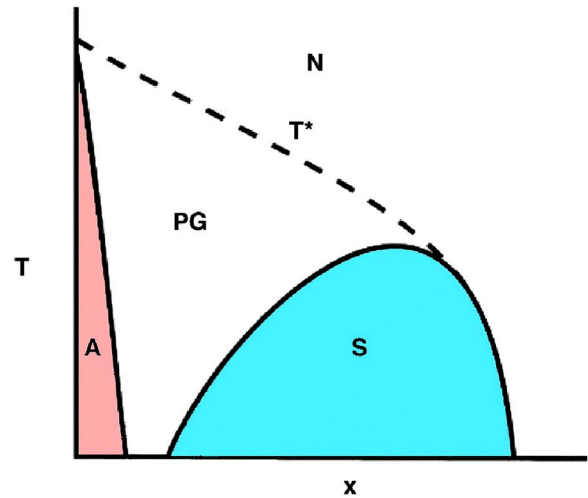


FIG. 7. (Color online) Schematic phase diagram of a hole-doped cuprate showing the superconducting (S), anti-ferromagnetic (A), and pseudogap (PG) regimes as a function of doping x . The dashed line labeled T^* designates the temperature at which the pseudogap opens.

temperature superconductors it is first necessary to understand the chemical doping of these compounds and certain aspects of their structure. Their carrier concentrations can be changed by chemical substitution of an insulating parent compound such as La_2CuO_4 , which on doping with Sr becomes $\text{La}_{2-x}\text{Sr}_x\text{CuO}_4$, or in compounds such as $(RE)\text{Ba}_2\text{Cu}_3\text{O}_{6+x}$, for which the doping level and carrier concentration are determined by the oxygen content x . (Here RE is one of the rare-earth elements.) At low doping levels, the compounds are antiferromagnetic insulators; at higher doping levels, they become superconductors. The transition temperature-doping relationship, which is illustrated in Fig. 7, is well characterized and is quite common. Crucially, the relevant range of carrier concentrations is small, roughly $0 < x \leq 0.2$ carrier per unit cell corresponding to an areal density $0 < n_{2d} \leq 10^{14} \text{ cm}^{-2}$ so that large changes in carrier concentration are not needed. The second attractive feature of high-temperature superconductors is the layered crystal structure, in which the key ingredient is believed to be the CuO_2 plane, a structurally robust feature whose properties, one may hope, are not strongly affected by the gate layer and the charge distribution.

The second feature of high-temperature superconductors that makes them attractive systems for FET doping is their layered crystal structures with electronic properties that are relatively insensitive to perturbations that do not affect the integrity of the electronically important CuO_2 planes.

There have been a number of successful electrostatic doping studies of high-temperature superconductors. Charge has been introduced by reversing the ferroelectric polarization of a layer of PZT ([Ahn *et al.*, 2003](#)), or through the use of an FET configuration with a high dielectric constant insulator ([Mannhart *et al.*, 1991](#); [Mannhart, 1996](#)). In the case of the former, analyses of

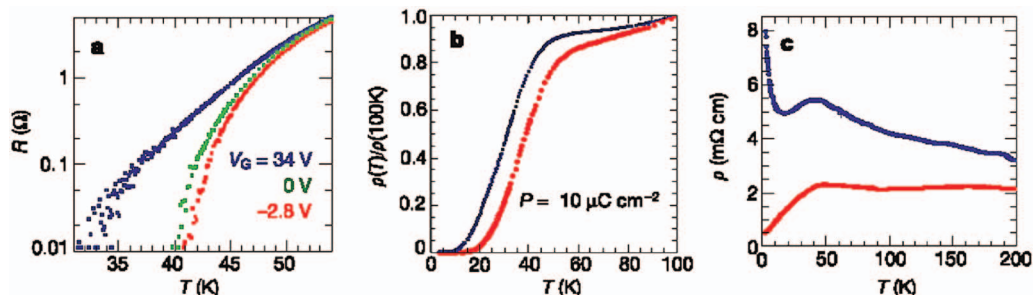


FIG. 8. (Color) Field effects in superconducting films: in each case, the blue curve corresponds to depletion of the carrier density and the red curve to enhancement of the carrier density in the source-drain channel. (a) Change of the dc resistance of an approximately 8-nm-thick $\text{YBa}_2\text{Cu}_3\text{O}_7$ channel with a 300-nm-thick $\text{Ba}_{0.15}\text{Sr}_{0.85}\text{TiO}_3$ gate insulator. The scatter in the data results from the noise of the measurement system. From Mannhart, 1996. The green curve in this panel shows the resistance with no field. (b) Resistance change of a 2-nm-thick $\text{GdBa}_2\text{Cu}_3\text{O}_{7-x}$ film induced by a 300-nm-thick PZT layer, with polarization P acting as a ferroelectric gate. The two curves have been normalized in the normal state. (c) Resistance change of a 2-nm-thick $\text{GdBa}_2\text{CuO}_{7-x}$ film whose doping level has been chosen to be close to the superconductor insulator transition, induced by a 300-nm-thick PZT layer acting as a ferroelectric gate. These data have been measured in a magnetic field of 1 T. From Ahn, Triscone, and Mannhart, 2003.

the resistivity variation upon polarization reversal as well as Hall-effect measurements show that the changes observed in the electronic properties were consistent with an alteration in the average carrier density equal to the measured polarization divided by the film thickness. Mannhart and Frey shifted the transition temperature of a $\text{YBa}_2\text{Cu}_3\text{O}_{7-\delta}$ film by 8 K [see Fig. 8(a)] (Mannhart, 1996). Matthey, Gariglio, and Triscone (2003) were able to enhance the superconducting transition temperature of a $\text{NdBa}_2\text{Cu}_3\text{O}_{7-\delta}$ film by 3.5 K in a configuration in which SrTiO_3 served as both the substrate and gate insulator. An enhancement of T_c was observed in a Ca -doped $\text{SmBa}_2\text{Cu}_3\text{O}_y$ film by the addition of electrons (Matijasevic *et al.*, 1994). See Fig. 8 for some examples of direct modulation of superconductivity. More recently Cassinese *et al.* (2004) and Salluzzo *et al.* (2004) described an FET device consisting of a $\text{Nd}_{1.2}\text{Ba}_{1.8}\text{Cu}_3\text{O}_x$ film grown on a (100) SrTiO_3 substrate, overlaid with an Al_2O_3 insulator and a Au gate. They demonstrated reversible changes of the hole density and were able to induce superconductivity in an insulating film that was eight unit cells in thickness. Parendo *et al.* (2005) were able to induce superconductivity electrostatically in amorphous Bi insulating films in a configuration in which a high dielectric constant material (SrTiO_3) served as both the substrate and gate insulator (Bhattacharya *et al.*, 2004a). In effect, in these experiments the ground state of a film was changed from insulating to superconducting by tuning an external parameter. In this instance the carrier density, in other words, the density modulation, induced a quantum phase transition (Sachdev, 1999).

The FET doping approach has been extended to other strongly correlated materials. Colossal magnetoresistance (CMR) manganites exhibit varying properties as the carrier concentration is changed, including formation and coexistence of ferromagnetic metallic, charge ordered antiferromagnetic insulating, and nonordered pseudogap phases (Uehara *et al.*, 1999; Tokura, 2000;

Salamon and Jaime, 2001). Field-effect experiments have shown reversible modulation of colossal magnetoresistance, revealing that charge modulation at fixed disorder influences the CMR effect (Tanaka *et al.*, 2002; Hong *et al.*, 2003, 2005). Unlike high- T_c materials, most of the CMR materials studied to date are electronically three dimensional, and with relatively short screening lengths, so that the induced charge is likely to be confined to within a few unit cells of the interface. The effect of this charge variation on the physical properties of the manganites is an open and interesting question.

In previous work on field-effect measurements in CMR materials, the resistance was found to change substantially upon gating (Wu *et al.*, 2001). This was done using films much thicker than the estimated Debye length, suggesting that effects other than straightforward charge modulation may be active. Recently films of $\text{La}_{0.8}\text{Ca}_{0.2}\text{MnO}_3$, a composition close to the phase boundary between a ferromagnetic metal and a charge ordered insulator, were grown on single-crystal SrTiO_3 substrates that had been thinned mechanically and provided with a gate on the back surface of the substrate (Bhattacharya *et al.*, 2004). The gate electric field was found to produce an ambipolar decrease in resistance at low temperatures attributed to the development of a pseudogap in the density of states (Eblen-Zayas *et al.*, 2005). The magnetic coercivity of a CMR material has also been shown to be altered electrostatically, although not reversibly (Bhattacharya *et al.*, 2005). Reversible tuning of the magnetic coercivity with a gate electric field was first demonstrated in the dilute magnetic semiconductor system $(\text{In},\text{Mn})\text{As}$ (Chiba *et al.*, 2003).

It has been possible to produce FET structures that are entirely of oxides (Mannhart *et al.*, 1991). We describe here the work of Ueno *et al.* (2003) in which a sputtered Al_2O_3 dielectric insulating layer was used to make FET devices on both undoped SrTiO_3 and KTaO_3 substrates by inducing charge at the interface between the insulating layer and perovskite. Although chemical

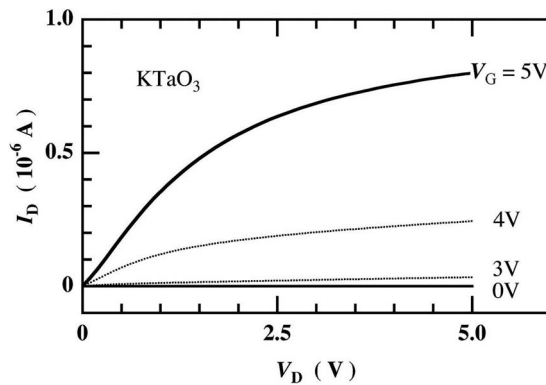


FIG. 9. Source-drain current-voltage characteristic of a KTaO_3 FET device at 300 K. The gate dielectric is Al_2O_3 .

doping that introduces electrons is known to induce semiconducting and eventually metallic behavior in KTaO_3 and SrTiO_3 [see, for example, [Leitner *et al.* \(1998\)](#)], in this instance the KTaO_3 and SrTiO_3 crystals are believed to be undoped band insulators. This work is important because it shows that it is possible to fabricate high-quality FET, including oxide layers with high breakdown voltages and negligible leakage current, and deliver large amounts of charge to the interface region. The structures were prepared by placing source and drain electrodes of Al on the (100) surface of these substrates. A 50-nm-thick amorphous Al_2O_3 film served as the insulator for the gate, and the gate itself was a layer of Au painted on the insulator. The average breakdown voltage of the Al_2O_3 films was 20 V, which corresponded to an electric field of 4 MV/cm, and the leakage current at breakdown was several nA over a $100 \times 400\text{-}\mu\text{m}^2$ area. The capacitance per unit area was $0.16\text{ }\mu\text{F}/\text{cm}^2$. Although there were serious attempts to optimize the properties of the Al_2O_3 layer, the maximum breakdown field never exceeded 10 MV/cm. The source-drain current-voltage characteristics of an Al_2O_3 - KTaO_3 FET were measured for different gate voltages. This device exhibited what appears to be typical *n*-channel FET behavior as shown in Fig. 9.

This behavior appears to be the same as that of a conventional Si MOSFET, but may be very different if the substrates are truly insulating with large band gaps. In conventional Si MOSFETs the electric field only modifies the charge distribution of a previously doped semiconductor. The SrTiO_3 and KTaO_3 substrates of these experiments are transparent, and little current flows between the source and drain electrodes without applying the gate electric field. The on-off ratios of these devices are in excess of 10^4 . The caveat is that despite all of this supporting evidence for different operation, it is, nevertheless, possible that carriers are doped into the perovskite during the deposition of the Al_2O_3 gate insulator. As a consequence, the nature of the operation of these devices is somewhat unsettled. Nevertheless, it is useful to employ similar technologies to electrostatically dope channels which are Mott insulating instead of band insulating, in an attempt to realize a gate-voltage-driven

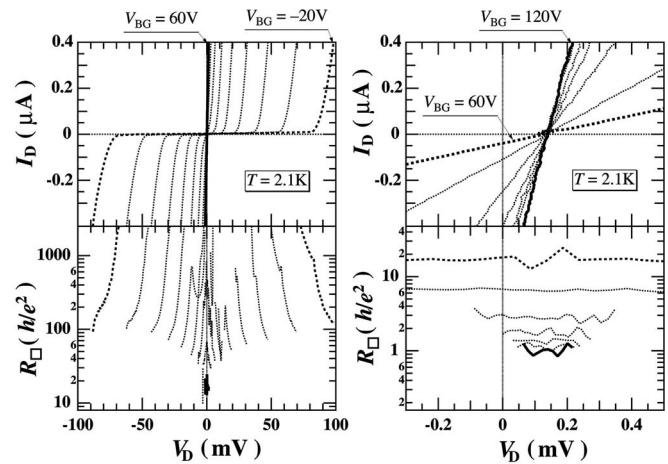


FIG. 10. Characteristics of an FET device involving accumulation of charge at the interface between a SrTiO_3 single crystal and a film of SrZrO_3 . Left top: The drain-source current I_D at 2.1 K plotted against the drain bias V_D . The experiment was done by scanning I_D from -0.4 to $0.4\text{ }\mu\text{A}$ while applying a gate voltage V_{BG} from -20 to 60 V. Left bottom: The sheet resistance R_{\square} in units of quantum resistance $h/e^2 = 25.8\text{ k}\Omega$. Right top: I_D - V_D for V_{BG} from 60 to 120 V. Right bottom: R_{\square} reaches as small as h/e^2 for V_{BG} of 120 V.

metal-insulator transition. This appears to have been achieved in certain oxide systems, and there have been a number of efforts directed at producing room-temperature oxide channel FETs that would exploit this phenomenon ([News *et al.*, 1998](#); [Ueno *et al.*, 2003, 2004](#), and for a recent review, see [Inoue, 2005](#)).

Another type of a gate-voltage-driven metal-insulator transition was reported by [Inoue *et al.* \(2004\)](#) at low temperatures in a two-dimensional system produced by accumulating charge electrostatically at the interface between a SrTiO_3 single crystal and a SrZrO_3 thin film. The interface was fabricated by heteroepitaxial deposition of a capping layer of three-unit-cell film of SrZrO_3 ($\sim 10\text{ }\text{\AA}$) on the step-and-terrace surface of SrTiO_3 using pulsed laser deposition, followed by sputter deposition of $1000\text{-}\text{\AA}$ -thick amorphous Al_2O_3 film which works in this case as a passivation layer. Drain and source electrodes with a channel length of $3\text{ }\mu\text{m}$ and channel width of $400\text{ }\mu\text{m}$ were made by evaporating Al metal into the trench formed by conventional Ar-ion-beam etching. The bottom of the electrode reached the $\text{SrZrO}_3/\text{SrTiO}_3$ interface.

The gate electric field V_{BG} was applied through the 0.5-mm -thick SrTiO_3 single crystal between the source-drain electrodes and a Au gate electrode which covers the whole area ($10 \times 10\text{ mm}^2$) of the back of the SrTiO_3 single crystal. Because of the large band gap difference (SrTiO_3 is about 3 eV, while SrZrO_3 6 eV), the carriers are considered to be accumulated mainly at the SrTiO_3 side of the interface.

A strong nonlinearity was observed in the current-voltage (I_D - V_D) curve at 2.1 K as shown in upper panels of Fig. 10. This *I*-*V* characteristic can be due to the back-

to-back formation of Schottky barriers at the source and drain electrodes. However, a simple one-step tunneling between the source and drain electrodes is ruled out because of the large channel length of $3\ \mu\text{m}$. A possible explanation for conduction is that microscopic charge inhomogeneities (charged domains) develop in the channel region in response to the gate electric field, and that transport is due to tunneling or hopping of carriers between these domains. When the gate electric field V_{BG} is increased, resulting in the accumulation of more charge at the $\text{SrZrO}_3/\text{SrTiO}_3$ interface, the gap in the I_D - V_D curve disappears dramatically and the curve becomes Ohmic. This occurs when the sheet resistance R_{\square} falls to the quantum resistance $h/e^2 = 25.8\ \text{k}\Omega$ at $V_{BG} = 120\ \text{V}$, where h is Planck's constant and e is the elementary charge. The fact that $R_{\square} \leq h/e^2$ together with the linearity of the I_D - V_D curve suggest that the interface area may have become metallic.

In this scenario for the insulator-to-metal transition in the two-dimensional system at the $\text{SrZrO}_3/\text{SrTiO}_3$ interface, the appearance of charge domains is concomitant with the collapse of Schottky barriers. We suggest that this can occur in transition-metal oxides because there exist competing ground states, which exhibit different types of order. The large fluctuations between these different ground states may give rise to microscopic inhomogeneities such as electronic phase separation. These inhomogeneities may be regarded as disadvantages if correlated materials are to be applied in electronics. However, if the electrostatic control of these inhomogeneities can be achieved in these correlated electron systems and understood, it may become an advantage, and its active utilization is a possible key to realizing conceptually new correlated electron devices operating in a completely different manner than conventional MOSFETs.

B. Scientific issues and challenges

Field-effect doping of novel materials raises important new issues of chemistry, physics, and materials science. In particular, the electronic properties of many novel materials are strongly affected by changes in local chemistry, in strain, and in disorder (Imada, Fujimori, and Tokura, 1998), so that an understanding of the physical and chemical structure of the interface is needed. Achieving the requisite characterization and control over FET structures is the key challenge to progress in this area. In the case of correlated oxides, it would be highly desirable to develop fabrication techniques that parallel those currently used for either GaAs or Si FETs.

For devices involving doping of correlated oxides, accumulation and depletion levels of the order of 10^{14} charges/ cm^2 are needed to modify the properties of the material (cf. Ahn *et al.*, 2003). Devices incorporating thin, high dielectric constant insulators allow this to be done at relatively low voltages $< 10\ \text{V}$; however, the effect of gate electrodes and induced carriers themselves are likely to produce significant effects.

A fundamental issue is that screening lengths are typically very short, so that the details of the interface become important. To see this, consider the charge distribution induced in a high- T_c superconductor by a voltage applied at an (001) interface. In high- T_c superconductors relevant electrons are tightly bound to weakly coupled, well-separated CuO_2 planes (Chu, 2002). We therefore idealize each plane as an infinitesimally thin but uniform charge sheet of areal density ρ_n , determined along with the electrochemical potential eV_n from

$$\rho_n = n(\mu_{\infty} + eV_n), \quad (4)$$

$$\frac{4\pi e}{\epsilon}(\rho_n - \rho_{\infty}) = \frac{V_{n+1} - 2V_n + V_{n-1}}{b}. \quad (5)$$

Here $\epsilon \sim 5$ – 10 (or much more in nearly ferroelectric materials such as SrTiO_3) is the background dielectric constant of the oxide, $b \sim 4\ \text{\AA}$ is the interplane spacing, μ_{∞} and ρ_{∞} are the electrochemical potential and electron density far from the interface, and $n(\mu)$ is the electron density given as a function of electrochemical potential.

The characteristic length scale of Eqs. (4) and (5) is the Thomas-Fermi length λ_{TF} which may be estimated by linearizing the equations in $\rho_n - \rho_{\infty}$ and assuming slow spatial variations. One finds

$$\lambda_{\text{TF}} = \sqrt{\epsilon b / (4\pi e^2 \partial n / \partial \mu)}. \quad (6)$$

These equations reveal the crucial role played by the chemical potential dependence of the density $n(\mu)$. In oxides, unlike in conventional semiconductors, $n(\mu)$ is expected to be controlled by correlation physics and is not well understood. A number of interesting theoretical proposals have been made (Vohllhardt, 1984; Furukawa and Imada, 1992; Moeller, 1995; Si and Varma, 1998); indeed one of the by-products of electric-field doping experiments may be a better understanding of this quantity. Further, in correlated oxides such as high- T_c superconductors, unlike conventional semiconductors, $\partial n / \partial \mu$ is believed to be large [a rough estimate comes from band theory, implying $\partial n / \partial \mu \sim 0.5$ – $1 / (\text{eV unit cell})$], yielding a Thomas-Fermi length of order the unit-cell dimension. In contrast to conventional Si FETs operating at carrier densities of 10^{12} – $10^{13}\ \text{cm}^{-2}$, where screening lengths are large, in correlated oxides the induced charge is concentrated within a few atomic layers of the surface. This estimate relies in an essential way on the weak interplane coupling of high- T_c superconductors, but more detailed analyses suggest that the basic orders of magnitude are similar in electronically three-dimensional correlated oxides (Okamoto and Millis, 2004a).

Thus, in correlated oxides, a clear understanding and precise control of the physical and chemical structure of the interface is crucial. Important issues include interface-induced physical changes in the structure (changes in bond lengths, atomic positions, and phonon frequencies), driven both by the presence of the gate layer and by the large electron density gradients near the interface, and interface-induced changes in the elec-

tronic structure. This latter problem although crucial to the understanding of the behavior of FET-doped systems, is as yet little studied. In a pioneering theoretical work, [Duffy and Stoneham \(1983\)](#) argued that changes in local environment could lead to significant changes in the many-body interaction parameters, and this effect was demonstrated experimentally by [Altieri *et al.* \(2002\)](#) in scattering studies of C_{60} films grown on different substrates. Important recent work on heterointerfacial layers has also been done by [Koerting *et al.* \(2005\)](#). The known sensitivity of the behavior of correlated electrons to small changes in parameters including charge density, strain, magnetic field, and chemical composition ([Millis, 2003](#)) suggests that changes in physical and electronic structure will lead to dramatic changes in near-surface collective behavior. [Warusawithana *et al.* \(2003\)](#) have shown that new kinds of collective order can appear at heterointerfaces.

Further development of theory is required in three areas. The first is a combination of band theory and quantum chemical calculations to provide information on the interface and electric-field-induced changes in electronic states and electronic structure; the second is more extensive many-body calculations to begin to explore the electronic phase reconstructions driven by these changes. Early attempts to study the second question in the context of model systems have appeared ([Potthoff and Nolting, 1999](#); [Liebsch, 2003](#); [Schweiger, Potthoff, and Nolting, 2003](#); [Okamoto and Millis, 2004a, 2004b, 2004c](#)) and have been compared to experiments on surfaces ([Maiti *et al.*, 1998](#)) and buried interfaces ([Ohtomo *et al.*, 2002](#)), and it seems likely that this area of research will grow rapidly in the future. A third important problem relates to the understanding of the chemical synthesis of heterointerfaces. They are formed using nonequilibrium growth processes in which chemical reactions are sequenced. In general, the best conditions for the growth of one slab will be different from the best conditions for the growth of the other one. In addition, the best condition for the synthesis of the interface can also be different. It has been found that heterovalent interfaces are more difficult to form than homovalent interfaces, but there is no theory to follow. Growth conditions are known to strongly affect the order at interfaces. How to control the conditions of surface chemical reactions in order to obtain the most ordered interface is a question theoretical chemistry should address. This would provide a new level of predictability for the multidimensional growth process and would help to distinguish fundamental phenomena from extrinsic effects.

Experimentally, there are many challenges to growing intrinsic interfaces and control of intrinsic behavior of collective states at such interfaces. Growth of an abrupt crystalline interface between the dielectric and field-modulated layer is particularly important for complex materials whose properties are sensitive to disorder. It is very helpful to have real-time analysis of the chemical reactions occurring during synthesis. Currently, reflection high-energy electron diffraction (RHEED) (see Fig.

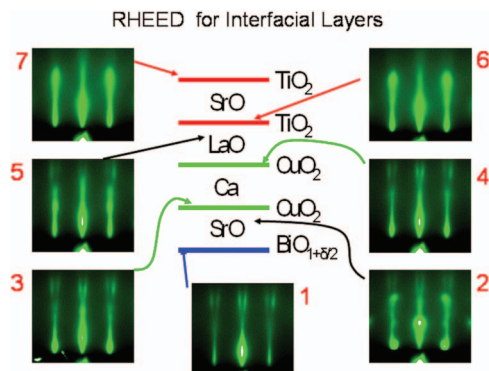


FIG. 11. (Color) RHEED patterns observed during epitaxial growth of field-effect doped CuO_2 planes. Interface layers are sequenced to be the natural layer stacking found in equilibrium phases.

11) is the most powerful tool in use in stand-alone synthesis chambers. As long as the surface is nearly flat, the specular reflection provides quantitative information regarding surface flatness, and the observation of transmission spots or diffuse reflection provides a measure of transient chemical intermediate states or surfaces with spoiled epitaxy, evidenced by the nucleation of second phase nanocrystals and atomic disorder, respectively. The difference between these two cases is found in the time history of the diffraction patterns observed. Figure 11 illustrates this for a particular atomic oxide layering architecture grown by molecular beam epitaxy (MBE) ([Oh *et al.*, 2004](#)). Panel 1 shows the diffraction pattern observed along the Cu-O bond direction after the completion of two BiO monolayers terminating a $Bi_2(La_xSr_{1-x})_2CaCu_2O_{8+\delta}$ molecular layer. The stretching of the specular reflection into a streak indicates a characteristic surface flatness length of ~ 40 nm. Panels 2 and 3 show that even during the growth of equilibrium phases intermediate surface states occur (panel 2) in which one component, in this case SrO , balls up into nanograins. But subsequent deposition of a monolayer of CuO_2 dissolves these grains and a smooth two-dimensional surface similar to that seen in panel 1 is obtained. In this experiment a junction between cuprate layers and an epitaxial insulator $SrTiO_3$ was formed using a monolayer of LaO at the interface, in order to provide the charge transfer required to put the top CuO_2 plane in an insulating state, free of holes. The RHEED images indicate a crystalline interface was grown. The scattered electrons, however, contain much more information and a theoretical effort to explore this by modeling should be undertaken.

An interesting experimental prospect would be the installation of an *in situ* MBE system at a synchrotron facility. Such a capability, movable between several end stations, would allow the whole range of scattering techniques including *in situ* photoemission to be applied to the problem of understanding how to achieve more perfect synthesis and properties of each atomic layer. In particular, this could be used to study how the electronic

structure and resulting collective behavior of field-effect doped layers evolve with thickness.

Further developing techniques to characterize the electronic or magnetic structure at buried interfaces of completed devices would be highly desirable. Recently there has been considerable progress on characterizing the performance of magnetic tunneling junctions. Yamada *et al.* (2004) have used nonlinear magneto-optical techniques, specifically magnetization-induced second harmonic generation, to probe interface magnetization. They have been able to optimize the interface to the perovskite ferromagnet $\text{La}_{0.6}\text{Sr}_{0.4}\text{MnO}_3$ with a nonmagnetic insulating layer as employed in spin-tunneling junctions. The use of this diagnostic was combined with tailored film growth using MBE techniques. This approach could also be used effectively to characterize magnetic interfaces in FET structures fabricated with magnetic materials. There would be considerable value in employing other approaches capable of probing buried interfaces, e.g., magneto-optical techniques such as circular magnetic dichroism and resonant x-ray scattering (Lussier *et al.*, 2002), or neutron reflectometry (Stahn *et al.*, 2005).

An advance in synthesis that could broadly impact the field would be incorporation of organic sources in a chamber connected to an oxide MBE system. This would allow interfaces between high dielectric constant layers and organic semiconductors to be formed without exposure of the dielectric interface layer, which contains the polarization charge, to air. This would eliminate the accumulation of potentially reactive water, CO_x , and organic layers from the interface between the two materials. Since the role of trapping defects in organic semiconductor transistors is known to be important, carefully controlling the synthesis of these interfaces using all *in situ* growth seems to be necessary. This would be a relatively simple step as multichamber MBE systems are commonly used when there is a need to incorporate chemically incompatible layers in single structures, or when one of the constituents of a particular structure is a “poison” for the growth of other constituents. Such a system would be useful in general for the integration of organic materials with oxides as might be needed for hybrid organic-inorganic electronics (Mitzi, Chondrous, and Kagan, 2001).

IV. ORGANIC SEMICONDUCTORS

A. Enabling experiments and technologies

Work on organic semiconductors is motivated by the potential development of plastic electronics. This is within the realm of possibility because organic materials can be processed at low temperatures (e.g., solution-based coating), which permits low-cost printing of electronic circuitry on large-area flexible substrates. One of the products of such technology might be an all-plastic roll-up display (Forest, 2004), with an organic thin-film transistor (OTFT) as the pixel-controlling element. Both inorganic and organic field-effect transistors operate in a

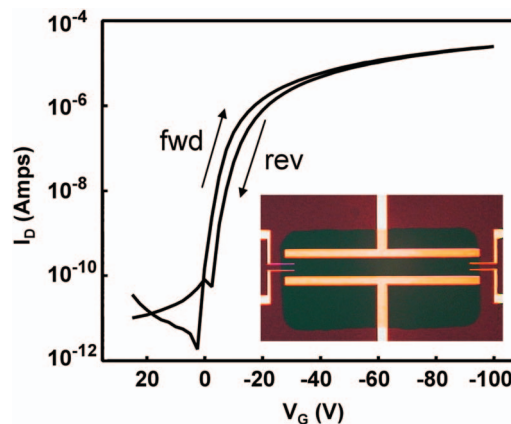


FIG. 12. (Color) The room-temperature I_D - V_G characteristic (transconductance) of a thin-film transistor based on a polycrystalline film of the organic semiconductor pentacene (the black patch of material). The gate dielectric is SiO_2 . The distance between the source and drain electrodes (large horizontal bars in the inset) is $200\ \mu\text{m}$. The hole mobility $\sim 1\ \text{cm}^2/\text{V}\cdot\text{s}$. The device turns on at negative gate voltages indicating hole conduction.

similar way: Application of a gate voltage induces a conducting channel at the interface between organic semiconductor and gate dielectric and reduces dramatically, by many orders of magnitude, the resistance between the source and drain contacts. However, the similarity stops here. The electronic properties of organic semiconductors are profoundly different from those of well-studied inorganic semiconductors such as Si and GaAs. Because of weak van der Waals bonding between molecules, the electronic bands in organic semiconductors are unusually narrow: a typical bandwidth $\sim 0.1\ \text{eV}$ is two orders of magnitude smaller than that in Si. The mobility of charge carriers, which are usually treated within the small-polaron model (Silinsh and Apek, 1994; Pope and Swenberg, 1999), is also much lower than in inorganic semiconductors. Unlike conventional Si MOSFETs, organic transistors are based on undoped organic semiconductors, so that charge in the channel originates in the source and drain contacts. The charge carriers are injected into the conduction channel from the metallic contacts, which have rather high resistance owing to a large potential barrier at the interface between an undoped semiconductor and a metal. An example of a drain current-gate voltage characteristic is shown in Fig. 12. It shows that the injection mechanism and contact current-voltage characteristics continue to be active areas of research (Bürgi *et al.*, 2002, 2003; Meijer *et al.*, 2003; Hamadani and Natelson, 2004; Pesavento *et al.*, 2004).

The sheet resistance of the conduction channel $R_{\square} = (en\mu)^{-1}$ is determined by the density of field-induced charges n and the charge-carrier mobility μ . The mobility in thin organic films has been increased dramatically over the past ten years due to the improved morphology of organic films. These films are either cast from solution or deposited from the vapor phase. They can be 100%

crystalline with grain sizes ranging from 100 nm to more than 10 μm depending on deposition conditions. In the best organic films (vapor-deposited pentacene), the mobility can be as high as 3 $\text{cm}^2/\text{V s}$ (Bulovic, Burrows, and Forest, 2000), which is comparable with that for the $\alpha\text{-Si:H}$ OTFTs commonly used in the active-matrix flat panel displays. [For a recent review on OTFTs, see Dimitrakopoulos and Mascaro (2001).]

The path to further improvement of OTFTs will involve perfection of organic semiconductor materials, as well as the development of new materials for the gate dielectric. For many OTFT demonstrations, the dielectric-gate assembly has been amorphous SiO_2 on Si, primarily because this is a readily available substrate. However, the oxide-coated Si wafers compromise the idea of low cost flexible electronics, and, consequently, there are growing efforts to identify suitable vapor- or solution-deposited polymeric gate dielectric materials. Two key considerations in dielectric selection are the dielectric properties (the dielectric constant and dielectric strength) and the density of defects at the interface between the gate dielectric and organic semiconductor. The density of states of organic materials studied by photoconductivity and optical absorption combined with FET properties has emerged as a useful diagnostic of defects near the interface between the oxide and insulator (Lang *et al.*, 2004a, 2004b).

Investigations of organic semiconductors have been focused on low-molecular-weight materials such as polyacenes. It is especially important to understand the physics of charge transport on the surface of these materials. The field-effect technique applied to single crystals rather than films is quite effective in addressing this issue: a relatively low density of surface states in weakly bonded organic molecular crystals facilitates observation of the field effect. The recent fabrication of field-effect structures using single crystals of organic materials has been an important step towards an understanding of intrinsic charge transport on organic surfaces. In the following we discuss several developments that have furthered the program of developing the science base of organic electronics. The developments include improvements in single-crystal growth technology and new approaches to developing field-effect structures on fragile organic surfaces, which have led to transistors with enhanced mobilities.

The ability to make organic single-crystal FETs hinges on the development of vapor phase growth techniques in the past two or three years. It has been possible using this approach to grow large free-standing single crystals of organic materials (up to 1 cm in the a - b crystallographic plane, but more typically a few mm) with a low surface trap density (e.g., $<10^{10} \text{ cm}^{-2}$). Vapor phase growth is relatively simple and large crystals can be produced in a matter of days.

The main obstacle to the realization of organic field-effect structures (OFETs) has been in the development of robust techniques to make field-effect structures on fragile organic surfaces without introducing a large density of surface defects. The solution has been nontrivial,

because conventional thin-film processing irreversibly damages surfaces of van der Waals bonded compounds. Two techniques of OFET fabrication have been successfully developed. The first approach is based on electrostatic bonding the surface of an organic film or crystal to a source-drain-gate structure that is prefabricated on a separate substrate (de Boer *et al.*, 2003; Takeya *et al.*, 2003; Sundar *et al.*, 2004). Two types of transistor stamps have been used so far: one based on conventional Si/ SiO_2 technology (de Boer *et al.*, 2003; Takeya *et al.*, 2003) and another one that uses flexible elastomer (PDMS) substrates (Sunder *et al.*, 2004). The process of lamination using a PDMS stamp is illustrated in Fig. 13. The second approach to forming FETs on the surface of organic crystals and films uses thin films of polymer parylene as the gate dielectric (Podzorov, Pudalov, and Gershenson, 2003). The interface between this polymer, deposited at room temperature onto the surface of a crystal or thin film, appears to have a low density of interface defect states.

Another major impediment to the realization of single-crystal OFETs is the lack of a heteroepitaxial growth technique for the van der Waals bonded organic films. In this situation, the only viable option to study the intrinsic charge transport on the surface of organic semiconductors is to fabricate field-effect structures on the surface of free-standing organic molecular crystals (OMCs). As emphasized above, this poses a serious technological challenge because these surfaces can be damaged much more easily than that of their inorganic counterpart. Also organic materials are largely incompatible with conventional microelectronic processing techniques such as sputtering, photolithography, etc. This is why the first single-crystal OFETs have been realized only recently (Butko *et al.*, 2003; de Boer *et al.*, 2003; Podzorov, Pudalov, and Gershenson, 2003; Podzorov, Sysoev, *et al.*, 2003; Takeya *et al.*, 2003; Hasegawa *et al.*, 2004). This remarkable progress is due to a number of novel fabrication schemes. Figure 14 shows the transconductance characteristic of an organic field-effect transistor fabricated on a single crystal of rubrene with a 1- μm -thick parylene gate dielectric. Higher mobilities have been achieved (up to 20 $\text{cm}^2/\text{V s}$) with rubrene transistors using air-gap stamps (Podzorov *et al.*, 2004a).

B. Scientific issues and challenges

The consistency of the experimental results obtained using single organic crystal FETs investigated by different research groups and fabricated by different techniques marks a critical step in the science of organic semiconductors. Such reproducibility has never been achieved in thin-film transistors that are known for their large spread of parameters, even in devices prepared under nominally identical conditions. Nevertheless, this first generation of organic single-crystal FETs is still affected by the presence of considerable imperfections that need to be eliminated.

The exponential decrease of the carrier mobility at low temperature points to the presence of substantial

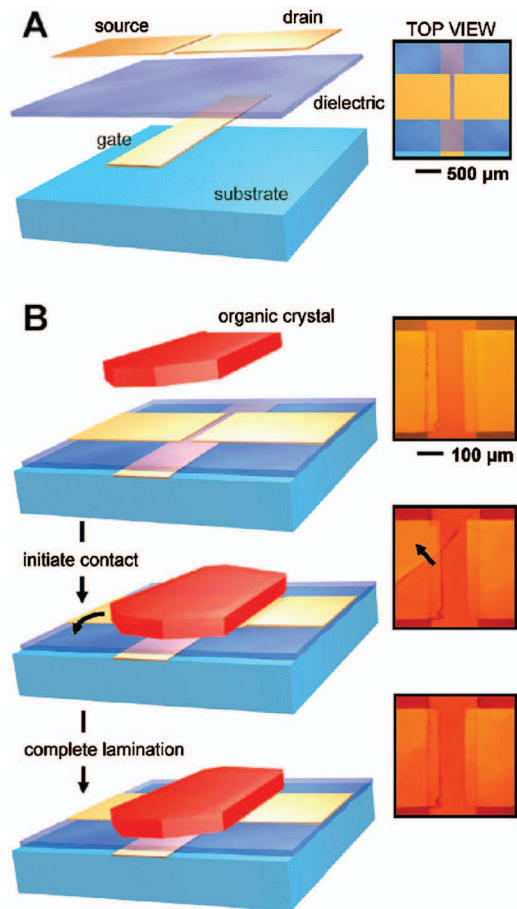


FIG. 13. (Color) Organic crystal transistor fabrication. (A) Schematic view of a transistor stamp on a PDMS substrate. (B) Transistor fabrication by lamination of an organic crystal against the transistor stamp. Initiating contact (first frame) between these two surfaces results in a wetting front that progresses across the semiconductor-stamp interface (second frame), until the entire crystal is in intimate contact with the stamp (final frame). The right insets show top views. From Sundar *et al.*, 2004.

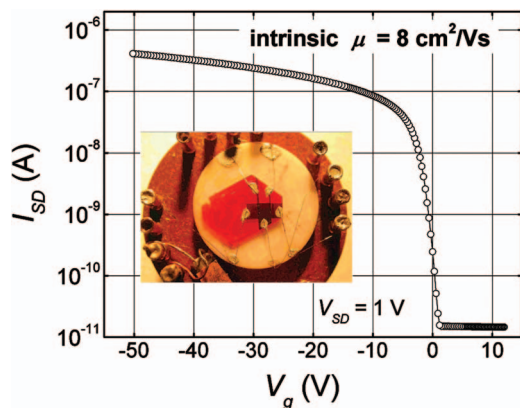


FIG. 14. (Color) The transconductance characteristic of an organic field-effect transistor fabricated on a single crystal of rubrene with a 1- μm -thick parylene gate dielectric. Rubrene crystals are typically a few mm across with the gap between source and drain contacts varying from 10 μm to a few hundred μm . The intrinsic mobility is the field-effect mobility. From Podzorov, Sysoev, *et al.*, 2003.

trapping. As single crystals are characterized by a high degree of structural perfection, chemical impurities are likely to be the dominating cause of trapping (Karl and Marktanner, 1998). For each molecular material of interest it is then necessary to understand what are the dominant molecular impurities and to decrease their concentration to the lowest possible level. Currently, there are no well-established methods that can be routinely used to achieve these goals and the development of new experimental techniques or the adaptation of techniques employed to study traps in Si is required.

The vapor phase transport technique that has been used to grow the organic crystals used in FETs can also be used to purify organic molecules. So far this technique has not been systematically optimized. Recent results indicate that significant increase in purity can be reached by keeping the molecular materials close to their sublimation temperature, in vacuum, for a sufficiently long period of time. It remains to be determined what is the ultimate level of purity that can be achieved in this way. A zone-refinement technique similar to that used to process Si can also be used for those organic materials that possess a coherent liquid phase (i.e., molecules that decompose at a temperature higher than their melting point). It is probably not a coincidence that the highest, low-temperature mobilities obtained in time-of-flight experiments have been observed in single crystals grown with zone-refined materials. It is also worth noting that the development of analytical tools and techniques that can be used to determine the chemical purity in this concentration range (estimated to be ~ 10 ppb in the purest zone-refined anthracene) will be required. Infrared spectroscopy, capable of identifying vibrational modes associated to specific chemical bonds, or photoluminescence experiments can be used as a starting point in this direction.

Other aspects of fundamental and applied relevance for organic FETs that need a systematic investigation concern the properties of the organic/dielectric and of the metal/organic interface (Scott, 2003). This is necessary in order to understand better the dynamics of charge injection at contacts. For disordered organic semiconductors such as polymers, charge injection seems to be diffusion limited (Hamadani and Natelson, 2004). However, a simple model of incorporating injection barriers is insufficient to explain the temperature dependence of the observed injection (Bürge *et al.*, 2003). For small organic molecules the situation is not clear, partially because of experimental irreproducibility originating from interfacial defects introduced during the contact fabrication. Recent progress, however, indicates that extrinsic effects can be overcome. It is worth noting that the issue of contact quality is also of direct relevance for thin-film devices. As these devices have normally a rather short channel (1–10 μm), contact effects can account for a large fraction of the device resistance and limit the device performance (i.e., on-off ratio, switching speed).

One specific aspect of contact between metallic electrodes and organic semiconductors that urgently re-

quires systematic investigation is the dependence of the contact resistance on the work function in metallic electrodes (Pesavento *et al.*, 2004). This dependence appears to be unexpectedly less crucial for organic semiconductors than for inorganic ones. This difference between organic and inorganic semiconductors may derive from different microscopic mechanisms responsible for charge injection at a metal/organic interface, which may not be as simple as the well-known Schottky barrier picture valid for inorganic semiconductors. Progress on this issue does not seem to be possible without systematic investigation performed on high-quality, well-characterized molecular systems. In terms of experimental configurations, this would mean deposition chambers with controlled vacuum environments in which traditionally incompatible materials (organic compounds and metals) could be deposited in a controlled manner.

In comparing the behavior of the contacts in inorganic and organic semiconductors, it should also be realized that in inorganic FETs heavy doping at the metallic electrodes is commonly used to suppress the contact resistance. In Si-based electronics, this is essential for many technological applications. A similar strategy cannot be presently implemented in molecular materials, since control of the doping level in these materials is outside the reach of current technology. Finding ways to introduce stable dopants into organic semiconductors without drastically altering the structural properties of the material is one of the outstanding challenges for future work in applied organic electronics. Research aiming at controlling chemical doping in organic materials also has the potential for a substantial impact in plastic electronics, an area which is already technologically significant.

In contrast with metal/organic interfaces, it seems that high-quality dielectric/organic interfaces can be obtained in single-crystal FETs in a rather reproducible way. High quality is suggested, among other things, by the behavior of the subthreshold slope which is often dominated by the quality of the contacts even in FETs with rather long channels (>1 mm). The development of experimental techniques for investigating the quality of buried interfaces, not presently available, is needed to reach a more quantitative understanding. This understanding (i.e., understanding the factors that determine the electronic quality of the organic/dielectric interface) is essential for the optimization of thin-film transistors, since in these devices the quality of the organic/dielectric interface critically determines the device behavior and is very sensitive to the fabrication process. It seems likely that improving thin-film devices will ultimately require the growth of crystalline organic films, where the structural order extends up to the first molecular layer in contact with the dielectric (since it is in this layer that most charge is accumulated during the FET operation). This presents a technological challenge for actual applications, as in this case the choice of the substrate material and of the organic film deposition technique may be restricted by different considerations.

This last point illustrates once again the more general issue of the relation between fundamental work and

practical device applications. An improved understanding of the intrinsic electronic properties of organic semiconductors, which will be achieved by investigating electrical transport through single-crystal devices, will be beneficial to understand the properties of applied devices based on thin films. Improving our fundamental knowledge will allow the selection of the most appropriate molecules for practical applications and may permit determining the ultimate limits of organic electronics. An even bigger impact on applications will be due to the technological progress originating from single-crystal work. The development of techniques for the purification of molecular materials can be directly used in the fabrication of thin-film devices and there is little doubt that this will result, for most materials, in an improvement of the charge carrier mobility. Similar considerations are relevant to techniques that will be developed for the fabrication of high-quality metallic electrical contacts or for other aspects of the FET fabrication. The use of parylene as a flexible gate insulator of exceptional quality illustrates this last statement. In short, an effective and rapid technological transfer between the work based on single-crystal and thin-film devices is highly beneficial at this time, which underscores the tight relationship between fundamental and applied research.

Future technological efforts will focus on a number of different issues. It is desirable to find new organic materials that are promising for single-crystal FET fabrication. Comparison between different (sufficiently pure) organic materials provides an effective tool to understand basic aspects of conduction in molecular crystals (e.g., the dependence on the molecular crystal structure). In addition, exploring a large range of materials facilitates the identification of molecules for which the carrier mobility is particularly high. Recent work on rubrene single-crystal FETs clearly illustrates this point. On the more technical side, experimental work will need to focus on a detailed comparison of transistor characteristics in devices fabricated with different techniques. This will lead to a deeper understanding of the functioning of organic transistors, which depends crucially on the electrical contacts and the dielectric/organic interface. Both issues are of fundamental interest (e.g., the physics of charge injection at a metal/organic interface is unknown) and of clear applied relevance.

Though the research on single-crystal organic transistors is less than five years old, the progress has been remarkably rapid. The technological advances have enabled realization of organic transistors with record parameters: the p -type mobility up to $20 \text{ cm}^2/\text{V s}$ at room temperature has been reported for rubrene OFETs, along with the $I_{\text{on}}/I_{\text{off}}$ in excess of 10^8 and the normalized subthreshold slope as small as $1.7 \text{ V nF/decade cm}^2$ (Podzorov, Sysoev, *et al.*, 2003; Sundar *et al.*, 2004). These parameters are an order of magnitude better than what has been achieved so far for the OTFT and α -Si:H FETs. However, it should be mentioned that single-crystal OFETs are not practical devices yet: there is a long way to go from these proof-of-concept experiments to the viable technology of single-crystal OFET

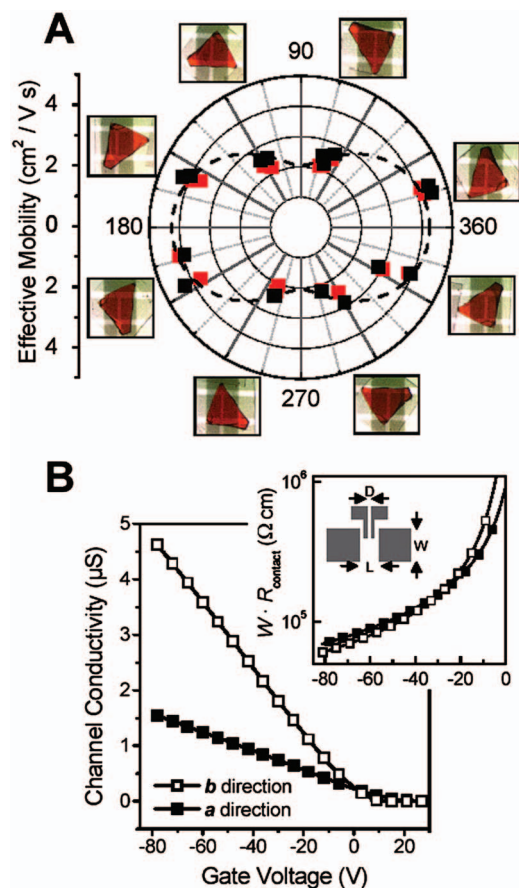


FIG. 15. (Color) Directional dependence of the mobility of rubrene crystals. (A) Polar plot of the mobility at the rubrene a - b surface (angle measured between the b axis and the direction of current flow). The maximum and minimum mobility values occur along b and a axes, respectively. (B) The four-probe measurements of the conductivity as a function of gate voltage along the b and a axes. Intrinsic mobilities measured along the b and a axes are 15.4 and 4.4 $\text{cm}^2/\text{V s}$, respectively.

fabrication that would be compatible with large-scale applications. At present, transferring the knowledge and technology developed from the study of single-crystal FETs to thin-film devices seems a more viable route to improve applied devices.

One of the important practical implications of single-crystal OFET fabrication is the opportunity to study the effect of molecular packing in organic crystals on carrier mobility. Indeed, the mobility of carriers in organic semiconductors depends critically on the intermolecular charge transfer in these strongly anisotropic materials. The anisotropy of charge transport has been well documented in the time-of-flight (TOF) experiments and, more recently, in experiments with rubrene FETs. Experiments with single-crystal OFETs facilitate testing of a wider variety of organic materials: such experiments do not require ultrapurification (as in the TOF experiments), or refinement of the thin-film deposition techniques (as in the OTFT experiments). Synthesis and identification of organic materials with high carrier mobility is an important direction of future research, which

requires combined efforts of chemists and physicists.

As far as the fundamental transport mechanisms in organic semiconductors are concerned, the intrinsic polaronic transport on the organic surface has been observed over a temperature range ~ 200 – 300 K. The signatures of this transport regime are (a) the mobility growth with cooling, and (b) the mobility anisotropy (see Fig. 15). In this respect, the OFET results are still less impressive than the results of the TOF experiments with bulk ultrapure crystals. However, taking into account that the transistor experiments address the charge transport on the surface, the realization of the intrinsic transport even over a limited temperature range can be considered as important progress. It also offers hope that with further technological advances intrinsic transport will be observed at lower temperatures—this will be crucial for realization of new phases driven by polaron-polaron interactions (it is worth emphasizing again that the FET experiments enable probing of the polaron densities by many orders of magnitude greater than in the TOF experiments).

V. INORGANIC LAYERED SEMICONDUCTORS

Recently, a new type of field-effect device involving the use of layered inorganic semiconductors has been introduced (Podzorov *et al.*, 2004b). The idea is to use a transition-metal dichalcogenide (TMD) as the active material for FETs. The transition-metal dichalcogenides belong to the class of layered inorganic semiconductors with a chemical formula MX_2 , where M stands for a transition metal and X stands for Se, S, or Te (Lieth, 1977; Bucher, 1992). The TMD crystals are formed by stacks of X - M - X layers. Atoms within each layer are held together by strong covalent-ionic mixed bonds, whereas the layers are weakly bonded to each other by van der Waals forces. Similar to graphite, the layered TMD can form nanostructures, such as fullerene-like nanoparticles (Tenne *et al.*, 1992), nanocrystals (Zhang *et al.*, 1996), and nanotubes (Remskar *et al.*, 2001). The semiconducting TMDs are considered to be promising materials for solar cells, photoelectrochemical cells, and p - n junctions (Späh *et al.*, 1983, 1985; Tenne and Wold, 1985).

Because of their layered structure, the TMD semiconductors are uniquely positioned for field-effect applications. These layered materials combine the advantages of organic and inorganic semiconductors, providing surfaces with an intrinsically low density of traps and high carrier mobility.

The transconductance characteristics of a WSe_2 FET device are shown in Fig. 16. Recent experiments (Podzorov *et al.*, 2004b) have demonstrated that the room-temperature carrier mobility in the TMD-based transistors can be very high (at least $500 \text{ cm}^2/\text{V s}$) due to the strong covalent bonding of atoms within the layers: this value is comparable to that for the best (nonflexible) Si MOSFETs and exceeds μ in organic and α -Si:H thin-film transistors (TFTs) by about two orders of magni-

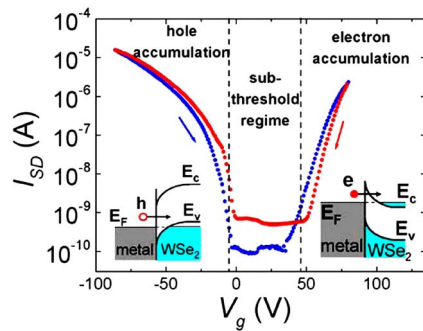


FIG. 16. (Color online) The transconductance characteristics of the WSe_2 FET measured at $T=60$ K. The observed hysteresis corresponds to sweeping V_g in the opposite directions shown by arrows ($V_g = +10$ V). The insets illustrate bending of the valence (E_V) and conduction (E_C) bands of the semiconductor at the interface with the injecting contact within the plane of the conduction channel; E_F is the Fermi level in this contact.

tude. The weak interlayer bonding results in an intrinsically low density of surface traps, and, thus, in a low field-effect threshold.

For applications it is crucial that metal chalcogenide films can be fabricated by the low-temperature spin-coating technique compatible with flexible substrates: the TFTs based on spin-coated SnSe_2 films exhibited n -type transport with mobility of the order of $10 \text{ cm}^2/\text{Vs}$ (Mitzi *et al.*, 2004).

Very recently, progress has been reported in the fabrication of field-effect devices based on individual (or small numbers of) graphene sheets (Berger *et al.*, 2004; Novoselov *et al.*, 2004; Bunch *et al.*, 2005; Zhang *et al.*, 2005). Since graphene is predicted to be a semimetal with carriers possessing a nearly linear dispersion $\epsilon(k) \sim k$, magnetotransport properties of these devices are expected to be rich. Very high room-temperature mobilities ($10^4 \text{ cm}^2/\text{Vs}$) have already been reported (Novoselov *et al.*, 2004).

The realization of FETs using inorganic layered semiconductors with a unique combination of characteristics (high mobility in combination with mechanical flexibility and ambipolar operation) might have a high impact on several fields of modern electronics. To bridge the gap between the proof-of-concept experiments that have been already done and the fabrication of viable devices, a wide range of fundamental issues needs to be addressed in future studies—from basic electronic processes in layered semiconductors, where the charge transport is confined within a few top layers, to mechanisms of the TMD doping. One of the essential steps towards commercialization of these devices would be development of the technique of epitaxial growth of single-crystal TMD films on various substrates, including flexible ones.

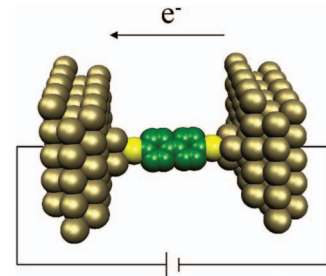


FIG. 17. (Color) Schematic of a molecular structure sandwiched between two bulk metallic electrodes. An additional gate electrode capacitively coupled to the molecule would be necessary for three-terminal experiments.

VI. SINGLE MOLECULES

A. Enabling experiments and technologies

Recent experimental investigations of gated electronic transport in molecular systems at the single nanometer scale have been enabled by advances in experimental techniques, particularly in device fabrication. Established methods exist for measuring two-terminal conduction through single (or small numbers of) molecules, including nanopores (Chen *et al.*, 1999), crossed wires (Collier *et al.*, 1999, 2000; Reed *et al.*, 2001; Zimmerman and Agnolet, 2001; Kushmerick *et al.*, 2002), mechanical break junctions (Ruitenbeek *et al.*, 1996; Reed *et al.*, 1997; Scheer *et al.*, 1998), scanning probe approaches with scanning tunneling microscopy (STM) (Joachim *et al.*, 1995; Yazdani, Eigler, and Lang, 1996; Datta *et al.*, 1997; Stipe *et al.*, 1998; Donhauser *et al.*, 2001; Reichert *et al.*, 2002; Smit *et al.*, 2002) or conducting probe atomic force microscopy (AFM) (Cui *et al.*, 2001; Wold and Frisbie, 2001; Ramachandran *et al.*, 2003). Extending these approaches to three-terminal devices has been extremely challenging because of geometrical and electrostatic constraints. Electrochemical gating of atomic-scale junctions and individual small molecules has also been demonstrated (Shu *et al.*, 2000; Chen, Zwolak, and Di Ventra, 2005; Xiao *et al.*, 2004, 2005; Albrecht *et al.*, 2005; Xu *et al.*, 2005a, 2005b).

We note that significant progress has been made in fabricating transistors based on carbon nanotubes. These macromolecules may be considered as one-dimensional semiconductor or metallic crystals, and exhibit a number of remarkable properties, including ballistic conduction. For a detailed review, see Dresselhaus, Dresselhaus, and Avouris (2000). In the following, however, we discuss devices based on single-nanometer-scale molecules rather than these macromolecular systems. A schematic of a single-molecule junction is shown in Fig. 17. Clearly it is unreasonable to expect such devices to act like standard MOSFETs. Modeling the channel like a classical electronic fluid that may be accumulated or depleted is manifestly unwise at the single-molecule scale. Nevertheless, these devices do function as transistors, with a third terminal capacitively modulating the electronic population of the channel and producing cor-

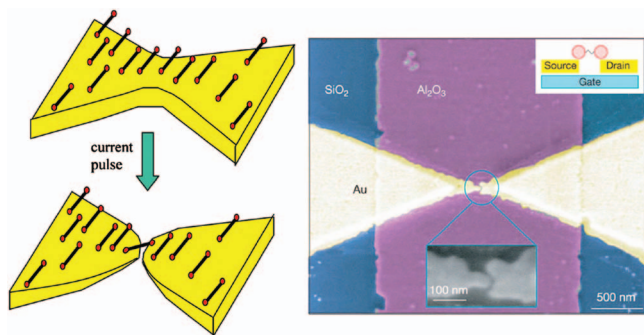


FIG. 18. (Color) Fabrication of single molecule transistors. Left: Schematic of electromigration technique [based on the approach of Park *et al.* (1999)] for fabricating single-molecule transistors. Prepatterned metal constrictions are decorated with molecules and then separated into distinct source and drain electrodes by electromigration in a cryogenic environment. Right: An electron micrograph of such a device, showing the underlying gate electrode. From Liang *et al.*, 2002.

responding changes in the source-drain conductance.

The particular method that has had the most success in producing functioning three-terminal nanometer-scale devices for the electrostatic tuning of single molecules is based on electromigration of lithographically defined constrictions in thin metal films (Park *et al.*, 1999) as shown in Fig. 18. These constrictions are typically separated from a gate electrode by a thin dielectric layer. The constrictions are decorated with molecules of interest (e.g., deposited by solution-based self-assembly), and are then placed in a cryostat and cooled to cryogenic temperatures. In the cryogenic UHV environment current is ramped through the constriction until electromigration breaks the metal into distinct source and drain electrodes separated by a nanometer-scale interelectrode gap.

All functioning molecular devices produced with this technique have performed as single-electron transistors (SETs) (Grabert and Devoret, 1992) with transport dominated by Coulomb blockade effects (Glazman, 2000). Single-electron transistors operate in a mode distinct from the conventional MOSFET and organic FETs discussed in previous sections. The channel is an island coupled to the source and drain electrodes by tunnel barriers. The island is sufficiently small that its single-particle level spectrum should be considered discrete rather than continuous. In equilibrium, single-particle states with energies below the chemical potential of the source or drain are filled, while higher energy states are empty. The energy required to promote an electron from the highest occupied island state, in a molecule, called HOMO, or highest occupied molecular orbital, to the lowest unoccupied island state, the LUMO, or lowest unoccupied molecular orbital, is Δ , the single-particle level spacing. Neglecting many-body effects, this is the energy of the lowest electron-hole excitation of the island. The energy required to add an additional electron to the island includes another contribution E_C , the Coulomb charging energy. An additional energy scale rel-

evant to electronic transport in this regime is Γ , the width of a given single-particle state of the island; this results from lifetime broadening of the island states due to couplings with the source and drain states. Clearly $\Gamma < \Delta$ is necessary for this description of the system in terms of island single-particle states to be physically relevant.

If the thermal energy scale $k_B T \ll \Delta$, E_C , and $\Gamma \ll E_C$ then the discrete island spectrum strongly affects electronic transport through the island. When this condition is fulfilled, and the chemical potential of the source or drain typically lies in the gap between occupied and unoccupied island levels, to first order no current may flow under an infinitesimal source-drain bias V_{SD} . In metal SETs, $E_C \gg \Delta$, and this suppression of conductance near $V_{SD}=0$ is called Coulomb blockade. The charging energy is typically approximated by that of a classical capacitor, with a total island capacitance including contributions from couplings to the source, the drain, and the gate.

The Coulomb blockade may be overcome either through increased $|V_{SD}|$ or by using a gate potential capacitively to shift the island single-particle states relative to the source-drain chemical potential. As a result, in the Coulomb blockade limit for $k_B T \ll E_C$, the conductance as a function V_G has periodic peaks that correspond to the energetic alignment of unoccupied island single-particle states with the source-drain chemical potential. Each such value of V_G corresponds to charge degeneracy, when two charge states of the island (differing by one electron) are energetically equal. For fixed V_G , the drain current I_D as a function of V_{SD} does *not* exhibit the saturation at large V_{SD} seen in conventional FETs.

Comparing energy scales immediately establishes that single molecule transistors (SMTs) operate in a completely different regime than most SETs. A typical all-metal SET will have $E_C \sim 0.5$ meV, $\Delta \sim 100$ meV. For a small SET defined in GaAs/AlGaAs two-dimensional electron gas, $E_C \sim 2$ meV, while $\Delta \sim 0.5$ meV. Smaller semiconductor quantum dots have been prepared, either from discrete semiconductor nanoparticles or by oxidation of nanopatterned Si wires, with resulting energy scales in the tens of meV. In a generic single-molecule transistor Δ , $E_C \sim$ hundreds of meV. The most important consequence of these comparatively enormous energy scales is that processes that are ordinarily irrelevant in SETs due to energy constraints (e.g., optical phonon emission and absorption) can have profound effects in SMTs.

A further difference between SMTs and nonmolecular devices is revealed by considering the effects of island charge on chemical stability. In a metal or semiconductor SET there are comparatively few restrictions (except for breakdown fields of dielectrics, for example) on the number of charge degeneracy points that may be explored. With a sufficiently large compensating gate voltage, any number of additional electrons may be added to a metal SET island one at a time by sweeping V_G to further positive potentials. However, chemical stability

imposes limits on the ability to add or remove electrons (reduce or oxidize, in chemical vernacular) from small molecules.

The comparatively large energy scales in SMTs imposed by confinement and Coulomb interactions have led to the observation of vibrational effects in SMT conduction. “Vibronic” resonances due to sequential tunneling through vibrationally excited molecular states have been observed (Park *et al.*, 2000, 2003; Yu and Natelson, 2004b; Yu *et al.*, 2004; Pasupathy *et al.*, 2005; Chae *et al.*, 2006; van der Zant *et al.*, 2006). Higher order inelastic tunneling features have also been reported (Yu *et al.*, 2004), and these are discussed further in the next section.

Conduction based on the Kondo effect is also relevant in SMTs. The Kondo effect is an archetypal many-body problem in which a localized spin degree of freedom becomes entangled with the spins of a conduction electron bath (Kondo, 1964). Because of on-site Coulomb repulsion, double occupation of the localized site is precluded; however, virtual processes result in an antiferromagnetic exchange between the spin and conduction electrons, with a characteristic energy scale given by T_K , the Kondo temperature. The ground state of this coupled system is a singlet, the formation of which is accompanied by an enhanced density of states at the Fermi level called the Kondo resonance.

Semiconductor quantum dots have proven extremely useful for studying the Kondo problem (Cronenwett, Oosterkamp, and Kouwenhoven, 1998; Goldhaber-Gordon *et al.*, 1998), since all parameters relevant to determining the Kondo state (the on-site repulsion energy; the difference in energy between the localized spin and the source-drain chemical potential; the lifetime broadening of the localized state) are tunable via gate voltages. The signature of the Kondo resonance in such three-terminal devices is a peak in the zero-bias differential conductance that appears for odd electron occupancy of the dot when $T \ll T_K$. In the zero-temperature limit for a dot symmetrically coupled to source and drain, the peak conductance in the Kondo regime reaches the unitary limit of $2e^2/h$. The peak is observed (van der Wiel *et al.*, 2000) to have a width in V_{SD} of approximately $2k_B T_K/e$.

Kondo conduction in SMTs has been reported by three groups in devices containing transition-metal complexes (Liang *et al.*, 2002; Park *et al.*, 2002; Yu *et al.*, 2005) and C_{60} (Pasupathy *et al.*, 2004; Yu and Natelson, 2004a, 2004b). Because of the comparatively large energy scales in the SMTs, the Kondo temperatures can be correspondingly higher, with T_K values reported in excess of liquid-nitrogen temperatures (Yu *et al.*, 2005). Given recent STM observations of transition-metal complexes on noble-metal surfaces with Kondo temperatures approaching 300 K (Wahl *et al.*, 2005; Zhao *et al.*, 2005), it is not unreasonable to consider SMTs operating in the Kondo regime at room temperature. There is evidence (via anomalous dependence of T_K on gate voltage), however, that Kondo physics in SMTs may require a more complex description than the comparatively

simple treatment that is so successful in semiconductor quantum dots (Yu *et al.*, 2005).

Single-molecule transistors also allow the measurement of Kondo systems with ferromagnetic leads (Pasupathy *et al.*, 2004). These devices can have very large magnetoresistive effects based on the relative magnetization orientations of the source and drain electrodes. Such Kondo systems with ferromagnetic electrodes have been the subject of a number of theoretical treatments (e.g., Sergueev *et al.*, 2002; Zhang *et al.*, 2002; Bulka and Lipinski, 2003; Lopez and Sanchez, 2003; Martinek *et al.*, 2003) and have been suggested as model systems for examining many-body physics relevant to quantum criticality (Kirchner *et al.*, 2005).

Kondo transport has also been observed in electromigrated junctions in the absence of molecules (Houck *et al.*, 2005; Heersche *et al.*, 2006). While the observation of Kondo physics in those cases depends crucially on the precise electromigration procedure, such experiments emphasize the importance of control experiments in SMT investigations. Improved fabrication and characterization methods would be most welcome.

It is worth considering whether single-molecule FETs are capable of operating in a mode similar to conventional FETs, rather than as Coulomb blockade devices. According to the simple picture discussed above, such operation would require either E_C or Δ values small compared to $k_B T$, or comparatively large Γ coefficients relative to the discretization of the molecular single-particle spectrum (good contacts). Even so, to achieve significant gate control of the channel potential in such a confined geometry, molecule-lead couplings would have to remain poor enough that screening in the molecule would be inferior to that in the metal source and drain electrodes. Such a conventional SMT has been realized recently by Tao and co-workers (Xu *et al.*, 2005a) using electrochemical gating. Transport in this regime may not be easily described with only few energy parameters. In very short molecules the broadening of molecular single-particle states induces a nonzero local density of states in the molecular region at the equilibrium chemical potential. The finite spatial distribution of these states in the molecule allows for direct tunneling from one electrode to the other, making transport similar to the one observed in resonant-tunneling devices. Details (in energy and real space) of the states induced by the molecule/electrode interface become important and microscopic theories (see below) are quite necessary to describe electron conduction. These issues become particularly relevant when localized interface states in the proximity of the molecule/electrode interface, and in the relevant energy range for scattering, are present. Charge transport then becomes a complicated function of the self-consistent charge redistribution under current flow. Analyses along these lines have been performed by several groups (Di Ventra *et al.*, 2000a; Lang and Solomon, 2005). We note that the extremely small molecular size and the resulting screening properties of highly discrete molecular spectra imply that conventional FET operation (e.g., saturation of drain current due to channel

pinch-off) is not relevant in these devices.

Because of the stochastic nature of the electromigration and molecule deposition processes, every SMT is different at the nanoscale. Device yields are typically reported to be $\sim 10\text{--}15\%$, with the remaining electrode pairs exhibiting transport characterized by no gate response (Yu and Natelson, 2004a, 2004b). Gate coupling of the SMT channel is generally poor compared to the source-drain coupling, presumably due to device geometry and screening effects of the source and drain electrodes. Accessing more than two charge states of a SMT is generally extremely challenging, even in devices incorporating ultrathin aluminum-oxide gate dielectrics (Park *et al.*, 2000, 2002; Liang *et al.*, 2002), though multiple accessible redox states have been reported in a related technique (Kubatkin *et al.*, 2003).

We note that the current lack of direct analytical techniques to probe the interelectrode gap at the atomic scale mandates a statistical approach to determining whether measured conduction results from individual molecules or other effects. One potential artifact of significant concern is the accidental formation, during junction fabrication, of metal nanoclusters (Yu and Natelson, 2004a, 2004b). In such a system, conduction can be a combination of intergrain and intermolecular tunneling, and Coulomb blockade via metallic grains (Zhitenev *et al.*, 2004). Another concern in nanojunction experiments is the adsorption of unintended contaminants during fabrication or measurement. As has long been known from scanning tunneling microscopy, surface adsorbates can significantly alter the conduction properties of a nanoscale junction (Lang and Avouris, 2002; Yang, Lang, and Di Ventra, 2003). This can be an issue in single-molecule transistor measurements, but may be mitigated through appropriate vacuum system and sample handling precautions. While there are techniques such as STM and nanotube-tip or chemical recognition AFM, none really have the necessary resolution or working conditions to examine the junction region directly. Clearly the development of better nanoscale probes of the junction region would enable much progress, as we discuss further below.

B. Scientific issues and challenges

There are a number of fundamental issues that need to be addressed relating to nanoscale structures, which may have an impact in future applications of molecular electronics. It is important to realize that there must be a natural (but so far unexplored) evolution of microscopic molecular material properties and concepts as the size or number of nanoscale components is increased from the single molecule limit to bulk molecular materials. Such a connection is not yet known and, if fully understood, it would allow us to progress considerably in this field.

A key and quite general issue, which affects single-molecule electronics as well, is the interaction between molecules and surfaces of metals and/or dielectrics. As has been shown to be the case for correlated oxides (Al-

tieri *et al.*, 2002) this interaction influences the charge transfer from or to the electrodes with consequent changes of electronic and transport properties. Such charge transfer can be easily modulated, for instance, by selectively choosing particular molecular terminating groups (Yaliraki *et al.*, 1999; Di Ventra and Lang, 2002; Patrone *et al.*, 2003). This suggests that tuning the conductance of these systems may be quite easy while severely constraining the experimental control of such structures. This also raises questions regarding the chemical doping of systems with such length scales: The charge transfer from or to the electrodes can be a substantial fraction of an electron charge. [See, for example, Ujsaghy *et al.* (2000), where charge transfer between a Au(111) surface and a physisorbed Co atom is approximately $1e^-$.] This already constitutes a sort of doping of the molecular structure (Di Ventra *et al.*, 2000b; Di Ventra and Lang, 2002). In addition, large differences in transport properties are expected when comparing chemisorption and physisorption of molecules on metal contacts. These differences reflect strong versus weak coupling of the isolated molecule electronic states to the electrode continuum of states. From simple electrostatics considerations, it appears that field-effect modification of the charge distribution in single-molecule devices is easier to achieve in the weak-coupling regime. However, gating effects in the strong-coupling regime could influence quantum interference effects between conducting channels thus leading to experimentally observable effects (Di Ventra *et al.*, 2000a; Yang, Lang, and Ventra, 2003; Xu *et al.*, 2005a). This is an area of research that has not been explored in depth. The different coupling strengths also influence the time electrons spend in the molecular junction (Nitzan, 2001) thus modifying electronic interactions with the molecular structure (electron-vibration coupling). In the weak-coupling limit, the average residence time of a carrier on the molecule is enhanced relative to the strong-coupling case; this may lead to relative enhancement of the coupling of charge and mechanical degrees of freedom of the molecule. A study of this transit time, while challenging to perform independent of other physics, would certainly shed new light on current-induced effects.

Other fundamental questions related to field-effect behavior of single molecules are the concept of capacitance and role of screening at the nanometer scale. The classical notion of capacitance at the molecular scale has to be replaced by a quantum-mechanical counterpart. Some ideas regarding this issue have been developed in mesoscopic physics (Buttiker, 2000) but further work has to be done in the present context. Similarly, systematic studies of screening and related issues have not yet been carried out. These issues are relevant, for instance, in understanding how impurities or surface states affect the conducting properties of single molecules. For instance, it has been shown (Lang and Avouris, 2002; Yang, Lang, and Di Ventra, 2003) that co-adsorption of impurities in proximity to a molecular junction can dramatically change its transport properties. This effect is partly due to electrostatic effects induced by the presence of the

impurities, and partly to the formation of bonds between the co-adsorbates and metal electrodes. Such bonds then act as extra scattering centers.

Electrical current can affect substantially the mechanical properties of a nanojunction. This is due to both atomistic rearrangements and diffusion of atoms due to the steady-state current density and to inelastic electron-phonon coupling. For instance it is well known that in metal nanowires substantial local heating of the structure can occur due to electron-phonon coupling (van den Brom, Yanson, and Ruitenbeek, 1998; Montgomery *et al.*, 2002; Yang *et al.*, 2005). Similar effects have been studied in single-molecule junctions (Chen, Zwolak, and Di Ventra, 2003; Troisi, Ratner, and Nitzan, 2003). Both current-induced forces and local heating can contribute to structural instabilities of molecular junctions, possibly at different ranges of the external bias (Yang *et al.*, 2005). These instabilities can pose severe limitations in the fabrication of reliable and reproducible devices. It is thus desirable to undertake a systematic study of these effects, in particular the relative role they play in a given nanostructure (Yang *et al.*, 2005). To stress even further the importance of heating in these structures, let us point out that, in general, in systems of nanoscale dimensions each electron, on average, releases only a small fraction of its energy to ions during the time it spends in the junction, making transport quasiballistic. However, the current density and, consequently, the power per atom are much larger in the junction compared to the bulk. This is at the origin of substantial local heating at very low voltages (Chen, Zwolak, and Di Ventra, 2005) as a direct consequence of the interplay between electron and phonon statistics. Dissipation of this heat away from the molecular junction into bulk electrodes is therefore an equally important issue. For instance, vibrational modes that are localized in the molecular region and are weakly coupled to the electrode phonon bath can easily appear in nanoscale systems (Montgomery and Todorov, 2003) (see Fig. 19). Such modes can be pumped by incoming electrons, making the structure unstable (Aji, Moore, and Varma, 2003; Chen, Zwolak, and Di Ventra, 2003; Mitra, Aleiner, and Millis, 2004). A thorough study of the steady-state temperature profile in nanoscale systems is thus necessary. This study would shed new light on the electron-phonon coupling in molecular systems as well as suggest ways to make these structures more stable under current flow. In addition, close to an electronic resonance, higher-order electron-phonon processes can contribute to specific inelastic features in the current-voltage characteristics (Galperin *et al.*, 2005) which can be observed with inelastic electron tunneling spectroscopy (IETS). This technique can also provide information on the actual geometry of a nanoscale junction, in particular its contact structure (Chen, Zwolak, and Di Ventra, 2004). Some IETS studies have been carried out on molecules on surfaces (Lorente *et al.*, 2001), but further work is needed (Stipe *et al.*, 1998, 1999; Luhon and Ho, 1999). Treating the weak-coupling regime requires a basic understanding of contact reconstruction and con-

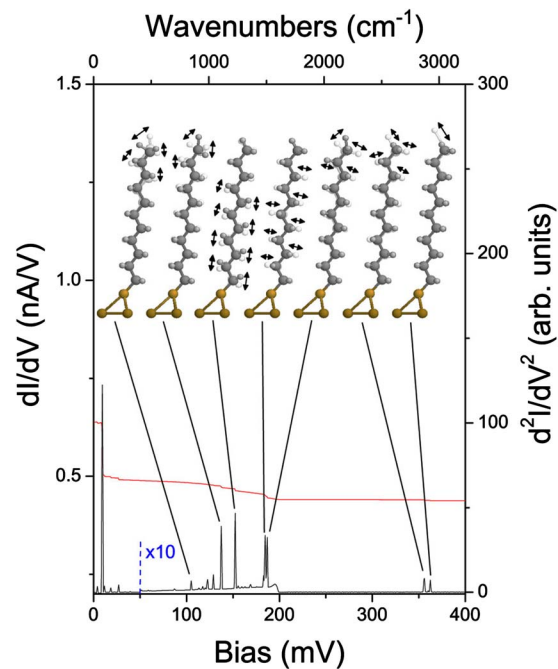


FIG. 19. (Color online) Differential conductance (left axis) and absolute value of the derivative of the conductance with respect to bias (right axis) as a function of bias for an undecanethiolate molecule between bulk electrodes. The schematics show some modes contributing to the inelastic features. Some of these modes have low coupling with the modes of the bulk electrodes. From Chen *et al.*, 2004.

formational changes due to the large fields generated between the source and drain electrodes. In the same vein, the role of a gate field in affecting the atomic geometry has not been explored. Recently IETS in nanoscale ensembles of molecules has been reported (Kushmerick *et al.*, 2004; Wang *et al.*, 2004). There have been a few experimental reports on Kondo-like physics in molecules (Liang *et al.*, 2002; Park *et al.*, 2002; Pasupathy *et al.*, 2004; Yu and Natelson, 2004a, 2004b) but it is not at all clear to what extent these interactions affect both the electronic spectrum and transport properties of the system, and, vice versa, how the atomic structure of a molecular junction determines the extent of electron-electron interactions. The study of electron interactions in single-molecule systems is much in its infancy. The gate dependence of IETS in single-molecule transistors (Yu *et al.*, 2004) has shown indications that the electron-vibrational coupling can be modified by gate tuning near molecular charge transitions. Nontrivial interplay between electronic correlations and vibrational effects have been suggested by several groups (Braig and Flensberg, 2003; Flensberg, 2003; Cornaglia, Ness, and Gempel, 2004; Mitra, Aleiner, and Millis, 2004).

The first experimental reports on transport in molecular junctions have sparked considerable theoretical efforts to understand the current-voltage characteristics of these systems. As previously discussed, details of the electronic and structural properties of the molecule-electrode interface have been found to be important so

that a large number of theoretical work has focused on the description of transport at the atomic level. Several theoretical techniques have been employed (Lang, 1995; Di Ventura and Lang, 2002; Xue, Datta, and Ratner, 2002; Baer and Neuhauser, 2003; Pecchia and Di Carlo, 2003) to solve the static scattering approach to electrical conduction. These can be grouped mainly into two sets: one that solves the Schrödinger equation in its integral form directly (the Lippman-Schwinger equation) and one that uses the nonequilibrium Green's function formalism (Keldish formalism). Apart from specific technicalities in their practical implementations and in absence of strong electron-electron interactions, both approaches describe the same physics. The common theme of these theoretical approaches is to use scattering potentials obtained from static density-functional theory (DFT) (Kohn and Sham, 1965). While this is of practical advantage, it is clearly not fundamentally correct: Static DFT is a theory of the ground state not suitable to describe nonequilibrium properties. This raises fundamental questions on the reliability of theoretical schemes based on static DFT, even in linear response (Sai *et al.*, 2005). In principle, a time-dependent formulation of the problem should be the natural way to address this issue (Di Ventura and Todorov, 2004; Burke *et al.*, 2005). However, it is not clear yet which theoretical approach is both rigorous and leads to a practical computational scheme. The use of the time-dependent formulation of DFT (Runge and Gross, 1984) in transport is still at its infancy and we believe that research in this direction is necessary. Such research can also unravel several fundamental issues related to the actual formulation of transport in atomic-scale conductors. For instance, a time-dependent study may allow the investigation of the onset, microscopic nature, and dependence on the initial conditions of steady states, the connection between different sources of noise, and possible variational properties of steady-state conduction (Di Ventura and Todorov, 2004).

Numerous experimental challenges exist when considering single-molecule field-effect experiments at the single-nanometer scale. Investigations at these length scales are in their infancy, and much room exists for improvement. Of particular importance are the difficulties of reproducible, well-controlled device fabrication. As has been described above, electronic transport at these scales is strongly influenced by charge transfer at interfaces. As a consequence the electronic structure of molecule-metal junctions can depend critically on the morphology and crystallographic orientation of the metal. Current approaches for fabricating three-terminal devices at these scales typically yield complicated metal morphologies, with the nanoscale electrode structure essentially a matter of chance determined by the microscopic details of polycrystalline physical vapor deposited metals. The challenge is twofold: to achieve reproducible contact morphology, and to assess the obtained configuration at the molecular scale.

As has been mentioned above, theory indicates that individual adsorbates near a molecular junction can strongly influence the resulting electronic transport. Per-

forming the device fabrication (e.g., electromigration) procedure and subsequent measurements in a cryogenic UHV environment can mitigate some concerns about unintentional adsorbates. However, particularly in measurements on molecules too large to be deposited by physical vapor deposition, one must be concerned about material and solvent purity, and the effects of co-adsorbed contaminants. While some molecular attachment schemes (thiol-based self-assembled monolayers) are believed to displace such contaminants, the surface environment local to the molecule of interest is currently impossible to assess directly in real devices due to a lack of appropriate analytical tools.

Currently no independent characterization techniques exist that can determine, *in situ*, the presence, orientation, bonding, or charge state of a single small molecule between nanospaced source and drain electrodes. While STM has proven incredibly useful for examining single molecules on clean metal surfaces, the geometry of SMTs is not amenable to such investigations. As a result this crucial information can only be inferred from indirect methods like transport measurements as a function of temperature, gate voltage, and source-drain bias. This is a severe limitation. Just as in larger organic devices, SMT investigations would be enhanced tremendously by the development of local diagnostic probes independent of electronic transport measurements.

Molecular sizes and level spacings are sufficiently large (~ 100 meV) that noncryogenic operations are conceivable. However, transport properties of SMTs are exponentially sensitive to 0.1-nm variations in device geometry, and the motion of molecules and metal atoms on surfaces at noncryogenic temperatures severely limits the temporal stability of current devices. The electrode morphology after electromigration is typically disordered and in a metastable state, subject to reconstruction and annealing upon thermal cycling. The irreversible structural changes and local defects associated with electromigrated electrodes can be significant obstacles to device measurements over broad ranges of temperature and bias voltage.

Similarly, the conductance of a single-electron device is sensitive to the local charge environment. Uncontrolled changes in the occupancy of traps near the active region of SMTs are of significant concern and must be controlled (see Fig. 20). Such traps could be present in the gate oxide, or could be surface states of the disordered source and drain electrodes. Many interesting studies on the effects of molecule-lead couplings on the electronic spectrum of SMTs are hampered by the relatively poor gate coupling necessitated by typical device geometries. Gate oxides that permit extremely large variations in the surface charge density near the molecules would be of great use, enhancing the accessibility of multiple charge states.

Just as in macroscopic devices based on molecular materials, the nature of the molecule-metal contact is currently far from clear in single-molecule devices. While thiol-based molecule attachment chemistries are

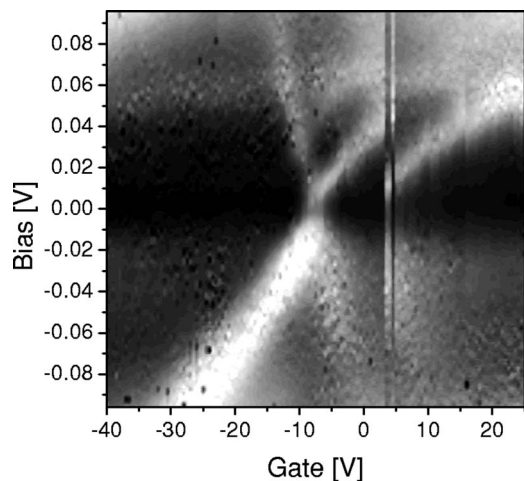


FIG. 20. Source-drain differential conductance map of a C_{60} -based single-molecule transistor showing an example of an instability (near 5-V gate voltage) due to an uncontrolled change in state of a nearby charge trap. From Yu and Natelson, 2004a.

popular, results indicate that SMTs are possible even in the absence of such chemical bonding.

VII. MAGNETIC SEMICONDUCTORS

The control of ferromagnetism using the electric-field effect has been demonstrated in several magnetic semiconductor materials. This was demonstrated first in III-V based InMnAs (Ohno *et al.*, 2000), and later in II-IV based MnGe (Park *et al.*, 2000) and II-VI based MnCdTe (Boukari *et al.*, 2002). In each instance electric-field control of ferromagnetism has been achieved using an insulating-gate field-effect transistor structure. Hole-induced ferromagnetism has been isothermally and reversibly varied.

The first work involved the use of (In,Mn)As, a ferromagnetic II-V semiconductor, which exhibits hole-induced ferromagnetism at relatively low carrier concentration. It is epitaxially grown within nonmagnetic InAs/(Al,Ga)Sb heterostructures. Manganese substitutes for indium in (In,Mn)As and provides localized magnetic moments and holes as it is an acceptor. The magnetic interaction between Mn ions is mediated by these holes, bringing about ferromagnetic order (Dietl *et al.*, 2000). The application of a negative gate voltage increases hole concentration, whereas positive gate voltage has an opposite effect. The former increases the magnetic coupling between localized Mn spins, whereas the latter decreases it.

Detecting the change of magnetization is complicated by the small dimensions of the devices studied along with the diamagnetism of the GaAs substrate, which would swamp the small ferromagnetic signal. Ohno *et al.* (2000) employed the anomalous Hall effect, which is sensitive to magnetization to sense the magnetic properties of the channel. The sheet Hall resistivity is given by the sum of the ordinary Hall effect and the anomalous

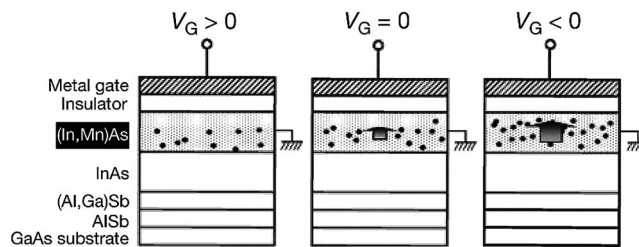


FIG. 21. Field-effect control of the hole-induced ferromagnetism in magnetic semiconductor (In,Mn)As field-effect transistors. Shown are the cross sections of a metal-insulator-semiconductor structure under various gate biases V_G . This controls the hole concentration in the magnetic semiconductor channel (solid circles). Negative gate bias increases hole concentration, leading to enhanced ferromagnetic interaction among magnetic Mn ions. Positive bias has the opposite effect. Arrows show schematically the magnitude of the Mn magnetization. From Ohno *et al.*, 2000.

Hall effect stemming from asymmetric scattering in the presence of magnetization. The Hall resistance R_H can be written as

$$R_H = (R_0/d)B + (R_S/d)M. \quad (7)$$

Here R_0 is the ordinary Hall coefficient, B and M are the magnetic field and magnetization perpendicular to the layer, R_S is the anomalous Hall coefficient, and d is the thickness of the channel.

In Fig. 21 we show a schematic of field-effect control of hole-induced ferromagnetism in one of these structures. In Fig. 22 we show the variation of R_H with magnetic field under different gate biases. There will be a spontaneous Hall resistance which is proportional to the

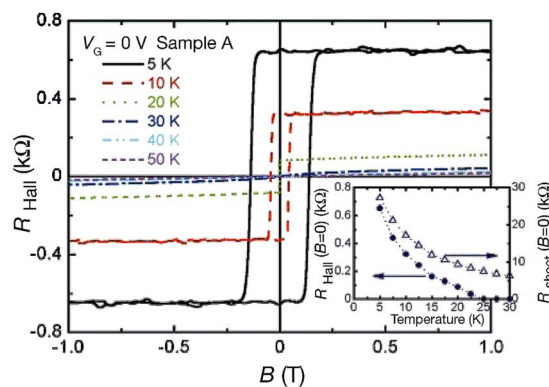


FIG. 22. (Color online) Magnetic-field dependence of the sheet Hall resistance R_{Hall} proportional to the magnetization of the magnetic semiconductor layer. R_{Hall} is used to measure the small magnetization of the channel. Shown are R_{Hall} as a function of field perpendicular to the layer at temperatures $T = 5$ – 50 K of one sample at $V_G = 0$ V. Clear hysteresis observed at $T \leq 20$ K is evidence of ferromagnetism. Inset: The temperature dependence of the remanence of R_{Hall} (solid circles), showing that the Curie temperature is above 20 K. Open circles indicate the channel sheet resistance R_{sheet} at zero field, which shows moderate negative temperature dependence. From Ohno *et al.*, 2000.

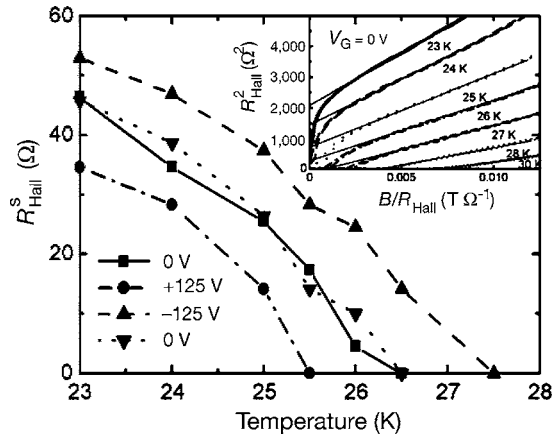


FIG. 23. Temperature dependence of the spontaneous Hall resistance R_{Hall}^S under three different values of V_G . R_{Hall}^S proportional to the spontaneous magnetization M_S indicates ± 1 -K modulation of T_C upon application of $V_G = \pm 125$ V. T_C is the temperature at which the spontaneous Hall resistance, and hence M_S , vanishes. Data at $V_G = 0$ V before and after application of ± 125 V are shown by squares and downward pointing triangles, respectively. In order to minimize the effect of domain rotation and magnetic anisotropy, the spontaneous Hall resistance is determined by extrapolation of R_{Hall} from moderate fields (0.1–0.7 T) to zero using Arrot plots (R_{Hall}^2 vs B/R_{Hall} plots shown in the inset). From [Ohno *et al.*, 2000](#).

spontaneous magnetization M_S . The Curie temperature is that at which M_S and the spontaneous Hall resistance falls to zero. These curves, shown in Fig. 23, demonstrate that an applied gate bias can change the Curie temperature and that ferromagnetism can be turned on and off with a gate.

The effect in the II-IV based magnetic semiconductor $\text{Mn}_x\text{Ge}_{1-x}$ is very similar. In this material, which is p type, there is again hole-mediated exchange. Magnetic ordering arises from long-range ferromagnetic interaction that dominates a short-range antiferromagnetic interaction. Here ferromagnetic order was modulated at higher temperatures, 50 K rather than 22 K, and smaller gate voltages (0.5 V as compared with 125 V) than required for InMnAs based devices. The implication is that electric-field controlled ferromagnetic order might be incorporated into conventional low voltage circuitry. The origin of the ferromagnetism in $\text{Mn}_x\text{Ge}_{1-x}$ was investigated using electronic structure calculations based on density-functional theory.

A third example of electric-field control of ferromagnetism in semiconductor heterostructures is the work of [Boukari *et al.* \(2002\)](#). In this instance a modulation-doped p -type $\text{Cd}_{0.96}\text{Mn}_{0.04}\text{Te}$ quantum well was placed in various built-in electric fields. Bias voltages generated isothermal and reversible crossovers between paramagnetic and ferromagnetic phases. This was also done by illumination by photons of energy greater than the band gap. The effects were carried out at a temperature of 1.3 K. Recently [Nazmul *et al.* \(2004\)](#) demonstrated control of magnetism in semiconductors at temperatures the order of 100 K in structures consisting of Mn δ -doped

GaAs and p -type AlGaAs, where the overlap of the hole wave function with the Mn δ -doping profile leads to high ferromagnetic Curie temperature. They were able to achieve a modulation of the Curie temperature as large as 15 K.

The practical application of tuning ferromagnetism requires that progress be made in the synthesis of room-temperature ferromagnetic semiconductors whose magnetic properties depend upon carrier concentration.

VIII. FUTURE RESEARCH OPPORTUNITIES

There are several future research opportunities that are available in correlated oxide systems. The ability to reversibly tune phase transitions in these strongly correlated systems may not only allow novel devices to be realized, but also provides new ways to investigate quantum critical phenomena, a subject of great current interest ([Sachdev, 1999](#)). Moreover, nanoscale manipulation of properties can be achieved using the electric-field-effect approach. Control of the ferroelectric polarization in ferroelectric or complex oxide heterostructures using scanning probe microscopy allows the generation of local-field effects in magnetic and superconducting oxides ([Ahn *et al.*, 1997](#); [Gariglio *et al.*, 2002](#)). This approach can be used for nanoscale control of correlated behavior to create artificial correlated structures within the plane of a material. Issues such as charge ordering and electronic phase separation may be amenable to study using the electric-field effect ([Ahn *et al.*, 2003](#); [Mathur and Littlewood, 2003](#)).

In highly polarizable crystals of organic semiconductors, strong electron-lattice coupling results in the formation of self-trapped electronic states with a size comparable to the lattice constant, the so-called small polarons ([Pope and Swenberg, 1999](#)). The polaronic effects shape both the dc transport and optical properties of these materials. Because of a very complicated character of the many-particle interactions involved in polaron formation, many fundamental issues remain poorly understood. Among them are (a) the effects of the molecular structure (intramolecular modes) and molecular packing (intermolecule modes) on the charge transport, (b) strong asymmetry in properties of negative and positive polaronic charge carriers, and (c) realization of coherent polaronic motion in extended states. Experiments performed in the past have not been capable of determining such important parameters as the concentration of mobile charge carriers, the effective mass, and the size of polaronic excitations, the characteristic energies involved in polaronic formation and polaron-polaron interactions.

The study of intrinsic (not limited by disorder) charge transport in these systems is hindered by very strong interactions of small polarons, the charge carriers with dimensions comparable to the lattice constant, with many types of lattice defects, including chemical impurities, vacancies, etc. Until recently, the intrinsic polaronic transport was observed only in the time-of-flight (TOF) experiments with bulk ultrapure organic crystals ([Karl,](#)

1999). These experiments established an important benchmark in our understanding of the charge transport in organic semiconductors. However, these experiments are limited in several respects. For instance, they tell us nothing about processes on the surface. Recent advances in fabrication of organic field-effect structures open a new avenue of the organic semiconductors research.

Development of single-crystal OFETs enables investigation of several aspects of the charge transport in organic materials that could not be addressed in the TOF experiments. In particular, the OFET-based experiments enable exploring much broader range of charge carrier densities, inaccessible in the TOF experiments. In this high-density regime, where accumulation of the order of one carrier per molecule seems to be feasible with the use of high- κ dielectrics, the polaron-polaron interactions play a major role; due to these interactions, realization of the new electronic phases might become possible. Indeed, it is known that at a sufficiently high density of chemically induced carriers, the potassium-doped fullerene K_xC_{60} exhibits superconductivity ($x=3$) and a Mott-Hubbard insulating state ($x=4$). This example illustrates a great potential of experiments with the single-crystal OFETs.

Though realization of the disorder-free transport is one of the primary goals of organic semiconductor research, the detailed characterization of interaction of polarons with crystal defects is equally important. Deeper understanding of interaction of polarons with defects will be crucial for the progress of organic electronics, in the direct analogy with the Si-based electronics, where realizing the importance of surface states by Bardeen in the late 1940s, and invention of the techniques for passivation of these states in the early 1960s (Riordan and Hodgeson, 1997) were two critical steps in developing Si MOSFETs. In this respect, development of new methods of trap spectroscopy in organic semiconductors seems to be very important.

Field-effect structures formed from layered inorganic semiconductors may be able to fulfill an important niche in modern electronics: the one in which there is a requirement for a combination of high charge carrier mobility (μ) and mechanical flexibility. Neither of the developed FETs satisfies these requirements. For example, the fabrication of silicon FETs with a relatively high $\mu \sim 200\text{--}400 \text{ cm}^2/\text{Vs}$ (Shur, 1990; Takagi *et al.*, 1994) is incompatible with flexible substrates. The organic-based FETs that provide basis for flexible electronics (Horowitz, 1998; Katz and Bao, 2000; Rogers *et al.*, 2001) are notoriously known for their low μ . Although several nanostructured materials have been recently considered for FETs (Buitelaar, Nussbaumer, and Schonberger, 2002; Smakov, Martin, and Balatsky, 2002; Avishai, Golub, and Zaikin, 2003) the demand for high-mobility flexible devices has not been satisfied.

Transition-metal dichalcogenide-based FETs can be bent without degradation of their characteristics. This mechanical flexibility of TMD-based FETs and a remarkably simple fabrication process (Podzorov *et al.*,

2004a, 2004b) make these devices very attractive for applications in the low-cost flexible electronics. Also, these transistors demonstrate ambipolar operation (very rare for high-mobility devices), which might be important for a broad range of applications, including light emission. Optimization of the performance and the development of simple fabrication techniques is an important direction for future research. Many of the problems encountered with correlated electron systems will also be relevant in this context.

There are several natural opportunities in the study of single-molecule devices. These involve a concerted effort combining theoretical and experimental research. To better control the resulting device properties, a systematic examination of the fabrication process and metal-molecule interface is a natural step. Variables available for control include source and drain electrode metal (particularly the work function), gate dielectric, and molecule termination chemistry (ranging from thiol-gold covalent bonding to van der Waals physisorption). These investigations will explore the effects of the molecule-metal interaction on electronic conduction, and may yield devices with improved stability as a function of time, bias, and temperature.

Another promising approach recently demonstrated would be the development of mechanical break junctions in a configuration that allows significant gate coupling. Two-terminal experiments (Smakov, Martin, and Balatsky, 2002; Champagne, Pasupathy, and Ralph, 2005) demonstrate the versatility of the tuning capability of break junctions, and gate-dependent studies of such systems would result in an improved understanding of metal-molecule contacts. Refinements of SMT fabrication methods that produce significantly increased device yields would be of great value, enabling far more studies than are currently possible.

The fabrication methods used to produce SMTs may also be applied to examine conduction on the single-nanometer scale in organic semiconductor devices of the type discussed earlier. Examining the nature of conduction in, e.g., rubrene or polythiophene as the channel size is increased from single molecules to the bulk limit would be a sensitive probe of the nature of conduction in such materials.

Given the early successes in implementing many-body correlated states in single-molecule devices (Liang *et al.*, 2002; Park *et al.*, 2002; Pasupathy *et al.*, 2004; Yu and Natelson, 2004a, 2004b) it is natural to examine such states in more detail. In particular, molecules with complicated internal spin structure due to their valence and ligand crystal fields are candidates for implementing novel quantum impurity problems. Similarly, a natural extension of present work would employ source and drain electrodes with nontrivial electronic correlations. Superconducting (Buitelaar, Nussbaumer, and Schonberger, 2002; Avishai, Golub, and Zaikin, 2003) and ferromagnetic (Pasupathy *et al.*, 2005) contacts to single molecules are likely to lead to rich physics in the Kondo regime.

In the longer term, scientific investigations of gated

single-molecule devices are likely to include measurements of higher correlations of electronic transport (e.g., noise and higher cumulants). Other areas likely to be explored are high-frequency dynamics (Kohler, Lehmann, and Hanggi, 2005), spin effects (Zwolak and Di Ventra, 2002), optical response, and quantum interference phenomena. Eventual applications of gated single-molecule devices are likely to be many years in the future, and would require significant advances in device yields, reproducibility, and stability. Sensor applications taking advantage of chemically specific binding are an example of a reasonable possible application.

In the case of magnetic semiconductors the size of the effects has been quite small. This is an area in which the development of new materials as with superconductivity may have a profound effect on future progress.

IX. DISCUSSION

The electrostatic modification of the electronic properties of materials is seen to have important consequences in the exploration of fundamental properties as well as the promise of new types of electronic devices for several rather different materials systems. The phase space of configurations that may be of interest is growing rapidly so that in a short introduction such as this one all possible configurations cannot be visited. It is quite clear that this is an active subfield of science that crosses several disciplines, with many challenges not yet met, but with substantial open opportunities.

ACKNOWLEDGMENTS

The authors would like to thank Professor C. P. Flynn for his encouragement during the course of this work. They would like to acknowledge the support of the Materials Council of the Department of Energy. The research of C.H.A. was supported by the AFOSR and by the National Science Foundation under Grant No. NSF-0134721, that of A.B., A.M.G., and C.D.F. by the University of Minnesota MRSEC (Grant No. NSF-0212032), and that of M.D.V. by Grant No. NSF-0133075, Grant No. NSF-0438018, and by the National Human Genome Research Institute. The research of J.N.E. was supported by the U.S. ONR Grant No. N00014-00-1-0840, that of M.E.G. by Grant No. NSF-0405208 and by Grant No. NSF-0437932, and that of J.M. by BMBF (Grant No. 13N6918), the DFG (Grant No. SFB484) and the ESF (THIOX). The research of A.J.M. was supported by the DOE (Grant No. ER46169), that of A.F.M. by FOM and by the NWO Vernieuwingsimpuls 2000, and that of D.N. by Grant No. NSF-0347253, the Robert Welch Foundation, and the David and Lucille Packard Foundation. The research of J.M.T. was supported by the Swiss National Science Foundation through the National Center of Competence in Research, "Materials with Novel Electronic Properties, MaNEP" and Division II, New Energy and Industrial Technology Development Organization (NEDO) of Japan, and ESF (THIOX). I.H.I.

was supported through the Correlated Electron Research Center.

REFERENCES

- Ahn, C. H., S. Gariglio, P. Paruch, T. Tybell, L. Antognazza, and J.-M. Triscone, 1999, *Science* **284**, 1152.
- Ahn, C. H., J.-M. Triscone, and J. Mannhart, 2003, *Nature (London)* **424**, 1015.
- Ahn, C. H., T. Tybell, L. Antognazza, K. Char, R. H. Hammond, M. R. Beasley, Ø. Fischer, and J. M. Triscone, 1997, *Science* **276**, 1100.
- Aji, V., J. E. Moore, and C. M. Varma, 2003, e-print cond-mat/0302222.
- Albrecht, T., A. Guckian, J. Ulstrup, and J. G. Vos, 2005, *Nano Lett.* **5**, 1451.
- Altieri, S., *et al.*, 2002, *Phys. Rev. B* **66**, 155432.
- Avishai, Y., A. Golub, and A. D. Zaikin, 2003, *Phys. Rev. B* **67**, 041301(R).
- Baer, R., and D. Neuhauser, 2003, *Int. J. Quantum Chem.* **1**, 524.
- Bednorz, J. G., and K. A. Müller, 1986, *Z. Phys. B: Condens. Matter* **64**, 189.
- Berger, C., *et al.*, 2004, e-print cond-mat/041240.
- Bhattacharya, A., *et al.*, 2004, *Appl. Phys. Lett.* **85**, 997.
- Bhattacharya, A., *et al.*, 2005, *Phys. Rev. B* **72**, 132406.
- Boukari, H., *et al.*, 2002, *Phys. Rev. Lett.* **88**, 207204.
- Bozovic, I., G. Logvenov, M. Verhoeven, P. Caputo, E. Goldobin, and M. R. Beasley, 2004, *Phys. Rev. Lett.* **93**, 157002.
- Braig, S., and K. Flensberg, 2003, *Phys. Rev. B* **68**, 205324.
- Bucher, E., 1992, in *Photoelectrochemistry and Photovoltaics of Layered Semiconductors*, edited by A. Aruchamy (Kluwer, Dordrecht), p. 1.
- Buitelaar, M. R., T. Nussbaumer, and C. Schonenberger, 2002, *Phys. Rev. Lett.* **89**, 256801.
- Bulka, B. R., and S. Lipinski, 2003, *Phys. Rev. B* **67**, 024404.
- Bulovic, V., P. E. Burrows, and S. R. Forrest, 2000, *Semicond. Semimetals* **64**, 255.
- Bunch, J. S., *et al.*, 2005, *Nano Lett.* **5**, 287.
- Bürgi, L., T. J. Richards, R. H. Friend, and H. Sirringhaus, 2003, *J. Appl. Phys.* **94**, 6129.
- Bürgi, L., H. Sirringhaus, and R. H. Friend, 2002, *Appl. Phys. Lett.* **80**, 2913.
- Burke, K., R. Car, and R. Gebauer, 2005, *Phys. Rev. Lett.* **94**, 146803.
- Butko, V. V., X. Chi, D. V. Lang, and A. P. Ramirez, 2003, *Appl. Phys. Lett.* **83**, 4773.
- Buttiker, M., 2000, *J. Low Temp. Phys.* **118**, 519.
- Cassinese, A., *et al.*, 2004, *Appl. Phys. Lett.* **84**, 3933.
- Chae, D.-H., J. F. Berry, S. Jung, F. A. Cotton, C. A. Murillo, and Z. Yao, 2006, *Nano Lett.* **6**, 165.
- Champagne, A. R., A. N. Pasupathy, and D. C. Ralph, 2005, *Nano Lett.* **5**, 305.
- Chen, F., *et al.*, 2004, *Nano Lett.* **5**, 503.
- Chen, J., *et al.*, 1999, *Science* **286**, 1550.
- Chen, Y. C., M. Zwolak, and M. Di Ventra, 2003, *Nano Lett.* **3**, 1691.
- Chen, Y. C., M. Zwolak, and M. Di Ventra, 2004, *Nano Lett.* **4**, 1709.
- Chen, Y. C., M. Zwolak, and M. Di Ventra, 2005, *Nano Lett.* **5**, 621.
- Chiba, D., M. Yamanouchi, F. Matsukura, and H. Ohno, 2003, *Science* **301**, 943.

- Chu, C. W., 2002, Phys. Scr., T **1102**, 40.
- Collier, C. P., *et al.*, 1999, Science **285**, 391.
- Collier, C. P., *et al.*, 2000, Science **289**, 1172.
- Cornaglia, P. S., H. Ness, and D. R. Grempel, 2004, Phys. Rev. Lett. **93**, 147201.
- Cronenwett, S. M., T. H. Oosterkamp, and L. P. Kouwenhoven, 1998, Nature (London) **281**, 540.
- Cui, X. D., *et al.*, 2001, Science **294**, 571.
- Datta, S., *et al.*, 1997, Phys. Rev. Lett. **79**, 2530.
- de Boer, R. W. I., A. F. Morpurgo, and T. M. Klapwijk, 2003, Appl. Phys. Lett. **83**, 4345.
- Dietl, T., *et al.*, 2000, Science **287**, 1019.
- Dimitrakopoulos, C. D., and D. J. Mascaró, 2001, IBM J. Res. Dev. **45**, 11.
- Di Ventura, M., and N. D. Lang, 2002, Phys. Rev. B **65**, 045402.
- Di Ventura, M., S. T. Pantelides, and N. D. Lang, 2000a, Appl. Phys. Lett. **76**, 3448.
- Di Ventura, M., S. T. Pantelides, and N. D. Lang, 2000b, Phys. Rev. Lett. **84**, 979.
- Di Ventura, M., and T. N. Todorov, 2004, J. Phys.: Condens. Matter **16**, 8025.
- Donhauser, Z. J., *et al.*, 2001, Science **292**, 2303.
- Dresselhaus, M. S., G. Dresselhaus, and Ph. Avouris, 2000, Eds., *Carbon Nanotubes: Synthesis, Structure, Properties, and Applications* (Springer-Verlag, Berlin).
- Duffy, D. M., and A. M. Stoneham, 1983, J. Phys. C **16**, 4087.
- Eblen-Zayas, M., *et al.*, 2005, Phys. Rev. Lett. **94**, 037204.
- Flensberg, K., 2003, Phys. Rev. B **68**, 205323.
- Forest, S. R., 2004, Nature (London) **428**, 911.
- Furukawa, N., and M. Imada, 1992, J. Phys. Soc. Jpn. **61**, 3331.
- Galperin, M., M. A. Ratner, and A. Nitzan, 2005, J. Chem. Phys. **121**, 11965.
- Gariglio, S., C. H. Ahn, D. Matthey, and J. M. Triscone, 2002, Phys. Rev. Lett. **88**, 067002.
- Glazman, L. I., 2000, Low Temp. Phys. **118**, 247.
- Goldhaber-Gordon, D., *et al.*, 1998, Nature (London) **391**, 156.
- Grabert, H., and M. H. Devoret, 1992, Eds., *Single Charge Tunneling, Coulomb Blockade Phenomena in Nanostructures*, Proceedings of a NATO Advanced Study Institute (Plenum, New York).
- Hamadani, B. H., and D. Natelson, 2004, Appl. Phys. Lett. **84**, 443.
- Hasegawa, T., K. Mattenberger, J. Takeya, and B. Batlogg, 2004, Phys. Rev. B **69**, 245115.
- Heersche, H. B., Z. de Groot, J. A. Folk, L. P. Kouwenhoven, H. S. J. van der Zant, A. A. Houck, J. Labaziewicz, and I. L. Chuang, 2006, Phys. Rev. Lett. **96**, 017205.
- Hong, X., A. Posadas, and C. H. Ahn, 2005, Appl. Phys. Lett. **86**, 142501.
- Hong, X., A. Posadas, A. Lin, and C. H. Ahn, 2003, Phys. Rev. B **68**, 134415.
- Horowitz, G., 1998, Adv. Mater. (Weinheim, Ger.) **10**, 365.
- Houck, A. A., J. Labaziewicz, E. K. Chan, J. A. Folk, and I. L. Chuang, 2005, Nano Lett. **5**, 1685.
- IBM, 2001, IBM J. Res. Dev. **45**, 3, available at <http://www.research.ibm.com/journal/rd45-1.html>
- Imada, M., A. Fujimori, and Y. Tokura, 1998, Rev. Mod. Phys. **70**, 1039; for additional reviews and perspectives see the special issue of Science, 2000, Science **482**, 460.
- Inoue, I. H., 2005, Semicond. Sci. Technol. **20**, S112.
- Inoue, I. H., *et al.*, 2004, preprint, available as part of the 2003 Annual Report of the Correlated Electron Research Center at <http://staff.aist.go.jp/i.inoue/papers/mine/CERC2004E.pdf>
- Izumi, M., *et al.*, 2001, Mater. Sci. Eng., B **84**, 53.
- Jerome, D., and L. G. Caron, 1987, *Low-Dimensional Conductors and Superconductors*, NATO Advanced Study Institute, Series B (Plenum, New York).
- Joachim, C., *et al.*, 1995, Phys. Rev. Lett. **74**, 2102.
- Karl, N., and J. Marktanner, 1998, Mol. Cryst. Liq. Cryst. Sci. (Switzerland) **314-315**, 465.
- Karl, N., *et al.*, 1999, J. Vac. Sci. Technol. A **17**, 2318.
- Katz, H. E., and Z. Bao, 2000, J. Phys. Chem. B **104**, 671.
- Kerting, V., *et al.*, 2005, Phys. Rev. B **71**, 104510.
- Kirchner, S., L. J. Zhu, Q. M. Si, and D. Natelson, 2005, Proc. Natl. Acad. Sci. U.S.A. **102**, 18824.
- Kohler, S., J. Lehmann, and P. Hanggi, 2005, Phys. Rep. **6**, 381.
- Kohn, W., and L. J. Sham, 1965, Phys. Rev. **140**, A1133.
- Kondo, J., 1964, Prog. Theor. Phys. **32**, 37.
- Kubatkin, S., *et al.*, 2003, Nature (London) **425**, 698.
- Kushmerick, J. G., J. Lazorick, C. H. Patterson, and R. Sashidar, 2004, Nano Lett. **4**, 639.
- Kushmerick, J. G., *et al.*, 2002, Phys. Rev. Lett. **89**, 086802.
- Lang, D. V., *et al.*, 2004a, Phys. Rev. Lett. **93**, 076601.
- Lang, D. V., *et al.*, 2004b, Phys. Rev. Lett. **93**, 086802.
- Lang, N. D., 1995, Phys. Rev. B **52**, 5335.
- Lang, N. D., and P. Avouris, 2002, Nano Lett. **2**, 1047.
- Lang, N. D., and P. M. Solomon, 2005, Nano Lett. **5**, 921.
- Lauhon, L. J., and W. Ho, 1999, Phys. Rev. B **60**, R8525.
- Leitner, Aronld, Charles T. Rogers, John C. Price, David A. Rudman, and David R. Herman, 1998, Appl. Phys. Lett. **72**, 3065.
- Liang, W., *et al.*, 2002, Nature (London) **417**, 725.
- Liebsch, A., 2003, Phys. Rev. Lett. **90**, 096401.
- Lieth, R. M. A., 1977, Ed., *Preparation and Crystal Growth of Materials with Layered Structures* (Reidel, Dordrecht).
- Lopez, R., and D. Sanchez, 2003, Phys. Rev. Lett. **90**, 116602.
- Lorente, N., M. Persson, L. J. Lauhon, and W. Ho, 2001, Phys. Rev. Lett. **86**, 2593.
- Lussier, A., *et al.*, 2002, J. Vac. Sci. Technol. B **20**, 1609.
- Maiti, K., P. Mahadevan, and D. D. Sarma, 1998, Phys. Rev. Lett. **80**, 2885.
- Mannhart, J., 1996, Supercond. Sci. Technol. **9**, 49.
- Mannhart, J., J. G. Bednorz, K. A. Müller, and D. G. Schlom, 1991, Z. Phys. B: Condens. Matter **83**, 307.
- Martinek, J., Y. Utsumi, H. Imamura, J. Barnas, S. Maekawa, J. König, and G. Schon, 2003, Phys. Rev. Lett. **91**, 127203.
- Mathur, N., and P. Littlewood, 2003, Phys. Today **56** (1), 25.
- Matijasevic, V. C., *et al.*, 1994, Physica C **235-240**, 2097.
- Matthey, D., S. Gariglio, and J.-M. Triscone, 2003, Appl. Phys. Lett. **83**, 3758.
- Meijer, E. J., *et al.*, 2003, Appl. Phys. Lett. **82**, 4576.
- Millis, A. J., 2003, Solid State Commun. **126**, 3.
- Mitra, A., I. Aleiner, and A. J. Millis, 2004, Phys. Rev. B **69**, 245302.
- Mitzi, D. B., K. Chondrous, and C. R. Kagan, 2001, IBM J. Res. Dev. **45**, 29.
- Mitzi, D. B., *et al.*, 2004, Nature (London) **428**, 299.
- Moeller, G., Q. Si, G. Kotliar, M. Rozenberg, and D. S. Fisher, 1995, Phys. Rev. Lett. **74**, 2082.
- Montgomery, M. J., and T. N. Todorov, 2003, J. Phys.: Condens. Matter **15**, 8781.
- Montgomery, M. J., T. N. Todorov, and A. P. Sutton, 2002, J. Phys.: Condens. Matter **14**, 5377.
- Nazmul, Ahsan M., S. Kobayashi, S. Sugahara, and M. Tanaka, 2004, Jpn. J. Appl. Phys., Part 2 **43**, 937.
- Newns, D. M., *et al.*, 1998, Appl. Phys. Lett. **73**, 780.

- Nitzan, A., 2001, *Annu. Rev. Phys. Chem.* **52**, 681.
- Novoselov, K. S., *et al.*, 2004, *Science* **306**, 666.
- Oh, S., M. Warusawithana, and J. N. Eckstein, 2004, *Phys. Rev. B* **70**, 064509.
- Ohno, H., D. Chiba, F. Matsukura, T. Omiya, E. Abe, T. Dietl, Y. Ohno, and K. Ohtani, 2000, *Nature (London)* **408**, 944.
- Ohtomo, M. D., A. B. Muller, D. Grezul, and H. Y. Hwang, 2002, *Nature (London)* **419**, 378.
- Okamoto, S., and A. J. Millis, 2004a, *Nature (London)* **428**, 630.
- Okamoto, S., and A. J. Millis, 2004b, *Phys. Rev. B* **70**, 075101.
- Okamoto, S., and A. J. Millis, 2004c, *Phys. Rev. B* **70**, 195120.
- Parendo, K., *et al.*, 2005, *Phys. Rev. Lett.* **95**, 049902(E).
- Park, H., *et al.*, 1999, *Appl. Phys. Lett.* **75**, 301.
- Park, H., *et al.*, 2000, *Nature (London)* **407**, 57.
- Park, J., *et al.*, 2002, *Nature (London)* **417**, 722.
- Park, J., *et al.*, 2003, *Thin Solid Films* **438-439**, 457.
- Park, Y. D., *et al.*, 2002, *Science* **295**, 651.
- Pasupathy, A. N., *et al.*, 2004, *Science* **306**, 86.
- Pasupathy, A. N., *et al.*, 2005, *Nano Lett.* **5**, 203.
- Patrone, L., *et al.*, 2003, *Phys. Rev. Lett.* **91**, 096802.
- Pecchia, Alessandro, and Aldo Di Carlo, 2003, *Rep. Prog. Phys.* **67**, 1497.
- Pesavento, P. V., R. J. Chesterfield, C. R. Newman, and C. D. Frisbie, 2004, *J. Appl. Phys.* **96**, 7312.
- Podzorov, V., V. M. Pudalov, and M. E. Gershenson, 2003, *Appl. Phys. Lett.* **82**, 1739.
- Podzorov, V., S. E. Sysoev, E. Loginova, V. M. Pudalov, and M. E. Gershenson, 2003, *Appl. Phys. Lett.* **83**, 3504.
- Podzorov, V., *et al.*, 2004a, *Phys. Rev. Lett.* **93**, 086602.
- Podzorov, V., *et al.*, 2004b, *Appl. Phys. Lett.* **84**, 3301.
- Pope, M., and C. E. Swenberg, 1999, *Electronic Processes in Organic Crystals and Polymers*, 2nd ed. (Oxford University Press, New York).
- Potthoff, M., and W. Nolting, 1999, *Phys. Rev. B* **60**, 7834.
- Ramachandran, G. K., *et al.*, 2003, *Science* **300**, 1413.
- Reed, M. A., *et al.*, 1997, *Science* **278**, 252.
- Reed, M. A., *et al.*, 2001, *Appl. Phys. Lett.* **78**, 3735.
- Reichert, J., *et al.*, 2002, *Phys. Rev. Lett.* **88**, 176804.
- Remskar, M., *et al.*, 2001, *Science* **292**, 479.
- Riordan, M., and L. Hoddeson, 1997, *Crystal Fire: The Birth of the Information Age* (Norton, New York).
- Rogers, J. A., *et al.*, 2001, *Proc. Natl. Acad. Sci. U.S.A.* **98**, 4835.
- Ruitenbeek, J. M. v., *et al.*, 1996, *Rev. Sci. Instrum.* **67**, 108.
- Runge, E., and E. K. U. Gross, 1984, *Phys. Rev. Lett.* **52**, 997.
- Sachdev, S., 1999, *Quantum Phase Transitions* (Cambridge University Press, Cambridge, England).
- Sai, N., M. Zwolak, G. Vignale, and M. DiVentra, 2005, *Phys. Rev. Lett.* **94**, 186810.
- Salamon, M. B., and M. Jaime, 2001, *Rev. Mod. Phys.* **73**, 583.
- Salluzzo, M., A. Cassinese, G. M. De Luca, A. Gambardella, A. Prigobbo, and R. Vaglio, 2004, *Phys. Rev. B* **70**, 214528.
- Scheer, E., *et al.*, 1998, *Nature (London)* **394**, 154.
- Schwieger, S., M. Potthoff, and W. Nolting, 2003, *Phys. Rev. B* **67**, 165408.
- Scott, J. C., 2003, *J. Vac. Sci. Technol. A* **21**, 521.
- Sergueev, N., Q. F. Sun, H. Guo, B. G. Wang, and J. Wang, 2002, *Phys. Rev. B* **65**, 165303.
- Shu, C., *et al.*, 2000, *Phys. Rev. Lett.* **84**, 5196.
- Shur, M., 1990, *Physics of Semiconductor Devices* (Prentice-Hall, Englewood Cliffs, NJ).
- Si, Q., and C. M. Varma, 1998, *Phys. Rev. Lett.* **81**, 4951.
- Silinish, E. A., and V. Apek, 1994, *Organic Molecular Crystals: Interaction, Localization, and Transport Phenomena* (AIP, New York).
- Smakov, J., I. Martin, and A. Balatsky, 2002, *Phys. Rev. Lett.* **88**, 037003.
- Smit, R. H. M., *et al.*, 2002, *Nature (London)* **419**, 906.
- Späh, R., *et al.*, 1983, *Appl. Phys. Lett.* **43**, 79.
- Späh, R., *et al.*, 1985, *Appl. Phys. Lett.* **47**, 871.
- Stahn, J., *et al.*, 2005, *Phys. Rev. B* **71**, 140509(R).
- Stipe, B. C., M. A. Rezaei, and W. Ho, 1998, *Science* **280**, 1732.
- Stipe, B. C., M. A. Rezaei, and W. Ho, 1999, *Phys. Rev. Lett.* **82**, 1724.
- Sundar, V. S., *et al.*, 2004, *Science* **303**, 1644.
- Sze, S. M., 1981, *Physics of Semiconductor Devices* (Wiley-Interscience, New York).
- Takagi, S., A. Toriumi, M. Iwase, and H. Tango, 1994, *IEEE Trans. Electron Devices* **41**, 2357.
- Takeya, J., *et al.*, 2003, *J. Appl. Phys.* **94**, 5800.
- Tanaka, H., J. Zhang, and T. Kawai, 2002, *Phys. Rev. Lett.* **88**, 027204.
- Tenne, R., L. Margulis, M. Genut, and G. Hodes, 1992, *Nature (London)* **360**, 444.
- Tenne, R., and A. Wold, 1985, *Appl. Phys. Lett.* **47**, 707.
- Tokura, Y., 2000, Ed., *Colossal Magnetoresistive Oxides*, Advances in Condensed Matter Science Vol. 2 (Gordon and Breach, New York).
- Troisi, A., M. A. Ratner, and A. J. Nitzan, 2003, *Chem. Phys.* **118**, 6072.
- Uehara, M., S. Mori, C. H. Chen, and S. W. Cheong, 1999, *Nature (London)* **399**, 560.
- Ueno, K., I. H. Inoue, H. Akoh, M. Kawasaki, Y. Tokura, and H. Takagi, 2003, *Appl. Phys. Lett.* **83**, 1755.
- Ueno, K., I. H. Inoue, T. Yamada, H. Akoh, Y. Tokura, and H. Takagi, 2004, *Appl. Phys. Lett.* **84**, 3726.
- Ujsaghy, O., J. Kroha, L. Szinyogh, and A. Zawadowski, 2000, *Phys. Rev. Lett.* **85**, 2557.
- van den Brom, H. E., A. I. Yanson, and J. M. van Ruitenbeek, 1998, *Physica B* **252**, 69.
- van der Wiel, W. G., S. De Franceschi, T. Fujisawa, J. M. Elzerman, S. Tarucha, and L. P. Kouwenhoven, 2000, *Science* **289**, 2105.
- van der Zant, Herre S. J., Yann-Vai Kervennic, Menno Poot, Kevin O'Neill, Zeger de Groot, Jos M. Thijssen, Hubert B. Heersche, Nicolai Stuhr-Hansen, Thomas Bjørnholm, Daniel Vanmaekelbergh, Cornelis A. van Walree, and Leonardus W. Jenneskens, 2006, *Faraday Discuss.* **131**, 347.
- Vollhardt, D., 1984, *Rev. Mod. Phys.* **56**, 99.
- Wahl, P., L. Diekhoner, G. Wittich, L. Vitali, M. A. Schneider, and K. Kern, 2005, *Phys. Rev. Lett.* **95**, 166601.
- Wang, W., T. Lee, I. Kretschmar, and M. A. Reed, 2004, *Nano Lett.* **4**, 643.
- Warusawithana, Maitri, Eugene V. Colla, J. N. Eckstein, and M. B. Weissman, 2003, *Phys. Rev. Lett.* **90**, 036802.
- Wold, D. J., and C. D. Frisbie, 2001, *J. Am. Chem. Soc.* **123**, 5549.
- Wu, T., *et al.*, 2001, *Phys. Rev. Lett.* **86**, 5998.
- Xiao, X., L. A. Nagahara, A. M. Rawlett, and N. J. Tao, 2005, *J. Am. Chem. Soc.* **127**, 9235.
- Xiao, X. Y., B. Q. Xu, and N. J. Tao, 2004, *Nano Lett.* **4**, 267.
- Xu, B. Q., *et al.*, 2005a, *J. Am. Chem. Soc.* **127**, 2386.
- Xu, B. Q., *et al.*, 2005b, *Nano Lett.* **5**, 1491.
- Xue, Y. Q., S. Datta, and M. A. Ratner, 2002, *Chem. Phys.* **281**, 151.

- Yaliraki, S. N., *et al.*, 1999, *J. Am. Chem. Soc.* **121**, 3428.
- Yamada, Hiroyuki, *et al.*, 2004, *Science* **305**, 646.
- Yang, Z., M. Chshiev, M. Zwolak, Y.-C. Chen, and M. Di Ventra, 2005, *Phys. Rev. B* **71**, 041402(R).
- Yang, Z., N. D. Lang, and M. Di Ventra, 2003, *Appl. Phys. Lett.* **82**, 1938.
- Yazdani, A., D. M. Eigler, and N. D. Lang, 1996, *Science* **272**, 1921.
- Yu, L. H., Z. K. Keane, J. W. Ciszek, L. Cheng, J. M. Tour, T. Baruah, M. R. Pederson, and D. Natelson, 2005, *Phys. Rev. Lett.* **95**, 256803.
- Yu, L. H., and D. Natelson, 2004a, *Nano Lett.* **4**, 79.
- Yu, L. H., and D. Natelson, 2004b, *Nanotechnology* **15**, S517.
- Yu, L. H., *et al.*, 2004, *Phys. Rev. Lett.* **93**, 266802.
- Zhang, J., J. Liu, J. L. Huang, P. Kim, and C. M. Lieber, 1996, *Science* **274**, 757.
- Zhang, P., Q. K. Xue, Y. P. Wang, and X. C. Xie, 2002, *Phys. Rev. Lett.* **89**, 286803.
- Zhang, Y., J. P. Small, M. E. S. Amori, and P. Kim, 2005, *Phys. Rev. Lett.* **94**, 176803.
- Zhao, A., Q. Li, L. Chan, H. Xiang, W. Wang, S. Pan, B. Wang, X. Xiao, J. Yang, J. G. Hou, and Q. Zhu, 2005, *Science* **309**, 1542.
- Zhitenev, N. B., A. Erbe, and Z. Bao, 2004, *Phys. Rev. Lett.* **92**, 186805.
- Zimmerman, D. T., and G. Agnolet, 2001, *Rev. Sci. Instrum.* **72**, 1781.
- Zwolak, M., and M. Di Ventra, 2002, *Appl. Phys. Lett.* **81**, 925.